Dynamic Gate Configurations at Airports: A Network Optimization Approach

Thomas Hagspihl[a,c], Rainer Kolisch[a,d], Christian Ruf[a,e], and Sebastian Schiffels[b,f]

Abstract

We consider the configuration of airport gates with passenger boarding bridges. The set of aircraft types that can be serviced at a gate depends on the installed boarding bridge(s). For instance, the Airbus A380 can only be serviced at gates equipped with a passenger boarding bridge that is able to access its upper level. Given the dynamic development of both the number of aircraft movements and the fleet mix at airports, the recurring decision problem is to determine for each gate whether and when the passenger boarding bridge configuration should be changed. The objective is to minimize investment and operating costs associated with the bridges as well as penalty costs for aircraft which cannot be processed because gates that are equipped with adequate gate configurations are not available. We propose a mixed-integer model formulation and present its underlying network structure. To solve the problem, we employ a column generation based heuristic approach. We demonstrate the good performance of the heuristic in a computational study and present a detailed discussion of the decisions taken as part of a case study.

Keywords: Transportation; Airport Gate Configuration; Integer Programming; Column generation

[a]Technical University of Munich, TUM School of Management, Arcisstraße 21, 80333 Munich
[b]Lancaster University Management School, Campus in Leipzig, Nikolaistr. 10, 04109 Leipzig
[c]Corresponding author; thomas.hagspihl@tum.de
[d]rainer.kolisch@tum.de
[e]christian.d.ruf@googlemail.com
[f]s.schiffels@lancaster.ac.uk

1 Introduction

Airports operate in a highly competitive environment, and the efficient use of infrastructure is a key driver of success (e.g., Caves 1994, Dorndorf et al. 2007). This paper focuses on the infrastructure provided at the gates[1], which represent the interface between the terminal complex and the apron and where the aircraft are accommodated during their service time on the ground. Passengers need to be conveyed safely, comfortably and efficiently from the terminal building to the parked aircraft and vice versa. To facilitate these deplaning and boarding operations, so called *passenger boarding bridges* (PBBs) are employed at the contact gates of most airports, especially large ones. For each gate, airports have to decide whether and, if so, how many PBBs of each type should be installed. We denote the resulting options - including the "no PBB" option - as *PBB configurations* that a contact parking position can be equipped with. The decision regarding which gate should be equipped with which PBB configuration depends on the aircraft types to be processed at the position in question, as the compatibility between aircraft types and PBB configurations is restricted by the various aircraft geometries (e.g., Kazda and Caves 2008). Thus, the decision of which PBB configuration to install at which gate clearly affects the gate capacity of an airport with respect to each aircraft type.

In addition to the compatibilities between aircraft types and PBB configurations, restrictions caused by the adjacent parking of aircraft have to be taken into account. The accommodation of an aircraft at a gate might be temporarily prohibited due to potential wingtip collisions with other aircraft parked at adjacent parking positions at the same time (cf. Dorndorf, Jaehn, and Pesch 2017). Also, so-called *Multi Aircraft Ramping Stands* (MARS) as proposed by International Air Transport Association (2004) and frequently employed at major airports need to be considered. Depending on their size, up to two aircraft can be accommodated simultaneously at a parking position configured as a MARS (which we will refer to in the following as a *MARS gate*). Due to their greater operational flexibility, MARS gates require special PBB configurations.

PBB configuration decisions have to be considered in a dynamic context, as the total number of aircraft present at an airport evolves over time, as does the fleet mix. This evolution may occur gradually or abruptly and may have either temporary or enduring effects. For instance, the average annual growth in global air traffic volume yields a gradual and enduring increase in traffic at many airports. One example of a gradual and permanent change in the fleet mix is the current trend towards employing smaller but more fuel efficient aircraft on long haul flights rather than large Boeing 747s or Airbus A380s (Boston Consulting Group 2020). It was in the course of this trend that both Airbus and Boeing recently announced that they would cease production of their largest aircraft models in the near future (Airbus 2019, Boeing 2020). An example of a sudden and permanent reduction in traffic volume at an airport is the opening of a new major airport in the vicinity. Finally, the current global crisis caused by the SARS-CoV-2 virus can be classified as an abrupt but temporary decline in air traffic volume. Adapting the gate capacity too early or too late

[1] In line with Dorndorf et al. (2007) and Ashford, Mumayiz, and Wright (2011), we will use the terms "gate" and "parking position" synonymously.

to a fluctuating traffic volume and fleet structure inevitably leads to either unused PBBs or aircraft which cannot be processed at a contact gate due to capacity shortages. Consequently, airports not only have to decide which PBB configuration should be installed at which parking position but also *when* - decisions that can be supported by various long-term forecasts that are regularly undertaken by important actors in the aviation industry (refer to Airbus 2018 or Eurocontrol 2018, for instance).

Facing a highly uncertain future, airport managers would prefer the most flexible PBB configurations over others if no further aspects were taken into account. However, higher flexibility is associated with higher cost, and decisions need to be considered carefully, as the cost of a single PBB is approximately $450,000$€ (Airport Improvement Magazine 2010, Travel PR News 2019). For instance, Terminal 1 at Munich Airport is currently undergoing expansion. Unaware of the aforementioned current development concerning the Airbus A380, decision makers at Munich Airport opted for two additional parking positions equipped with PBBs with sufficient flexibility for processing the A380 at the new terminal building (Munich Airport 2016). As the airport already possesses gates which can process the A380 in sufficient number to serve pre-SARS-CoV-2 traffic, it is at least questionable from today's point of view whether the investment in additional PBBs will eventually pay off.

The overall question is when to equip which gate with which PBB configuration, balancing the operational flexibility and total cost with respect to the PBB configurations. We propose a model to formally describe this problem. To increase the tractability of the problem, we propose a *Dantzig-Wolfe decomposition*, which exploits the inherent network structure. Based on a *column generation* methodology, we propose a heuristic solution approach to the problem and show that it performs well for realistic data instances.

The remainder of this paper is structured as follows: In Section 2, we position our work in the literature. Section 3 introduces the details of the problem. A mixed-integer model is presented in Section 4, while Section 5 describes our proposed solution approach. The computational study presented in Section 6 investigates the performance of the proposed procedure. In Section 7, we present a case study for Munich Airport Terminal 2, based on real data. Finally, conclusions and recommendations for future research are presented in Section 8.

2 Related Literature

Our work is positioned at the interface between the strategic capacity planning of aprons and the gate assignment problem (i.e., the optimal assignment of aircraft to gates). We will briefly discuss the existing literature from both fields of research and state the similarities and differences of both streams compared to our approach.

Strategic capacity planning of aprons. The strategic management of apron capacity has been addressed from different perspectives. An elaborate review of the relevant literature is provided

by Mirković and Tošić (2014). Simple formulas for calculating the capacity of a given apron can be found in Ashford, Mumayiz, and Wright (2011), Horonjeff et al. (2010), and de Neufville and Odoni (2013). These formulae either assume that each gate can accommodate all aircraft types or they take existing compatibility restrictions into account and calculate apron capacities for different types of aircraft. More elaborate methods provide advice on the number of gates an apron should have to be able to fulfill certain requirements, mostly under stochastic conditions (see Bandara and Wirasinghe 1989, Wirasinghe and Bandara 1990, Steuart 1974, Hassounah and Steuart 1993, Narciso and Piera 2015). Furthermore, comparing hub airports to non-hub airports, Mirković and Tošić (2017) demonstrate how gate capacity depends on the traffic characteristics of the airport.

This paper relates to the strategic planning of apron capacity, as the choice of PBB configurations at gates determines how many aircraft of each type can be served simultaneously. However, while the above literature provides formulae with which to perform a one-time calculation of apron capacity for the number of gates available, the objective of this work is to dynamically reconfigure the gates so as to enable the most cost-efficient use of the existing infrastructure in the long run[2]. We therefore investgate not only how much capacity of which type needs to be provided, but also when it is needed. Furthermore, existing work investigates the number of aircraft that a given apron can process per time unit considering a continuous time horizon of operational length. In contrast, we aim to dynamically adjust the number of aircraft which can be processed simultaneously (i.e., at a given moment in time) over a strategic time horizon. Finally, contrasting the existing literature, we consider such operational aspects as MARS gates and adjacency restrictions in our model.

Gate assignment problem. The second stream of research that our problem relates to is the gate assignment problem, where arriving aircraft need to be assigned to available, compatible gates. Extensive reviews of the literature considering this problem are provided by Dorndorf et al. (2007), Cheng, Ho, and Kwan (2012), Guépet et al. (2015), and recently by Daş, Gzara, and Stützle (2020). The main similarity of our approach to existing literature that discusses the gate assignment problem is that we assign aircraft to gates subject to capacity and compatibility constraints, while additionally considering aircraft parked at both adjacent gates and MARS gates. However, rather than creating a schedule for the operative level of decision making, where individual aircraft are assigned to gates, we determine on a strategic level which type of aircraft each gate accommodates to enable long-term adaption of PBB configurations and in turn efficiently service the aggregate traffic. Our objective is thus to minimize the number of aircraft that cannot be accommodated at a contact gate due to gate unavailability or incompatibility. In contrast, existing literature on the gate assignment problem considers such objectives as the minimization of the total walking distance for passengers and the minimization of the number of required towing procedures or else attempts to find robust schedules that remain stable in the face of uncertainty. Daş, Gzara, and Stützle (2020) find that more recent approaches tend to incorporate multiple objectives. While the gate assignment problem itself has been proven to be NP-hard (Guépet et al. 2015), we employ a

[2]This follows the recommendations by Caves 1994 and Narciso and Piera 2015 to improve the efficiency of existing apron space instead of investing in new infrastructure.

basic version of it embedded into our strategic decision problem.

3 Problem Description

We consider the PBBs at the contact gates of an airport over a strategic time horizon of up to 10 years. Time is discretized into periods with a length of half a year each, as this interval matches the seasons over which flight plans generally remain unchanged and thus the capacity requirements posed to airports remain stable. The objective is to strike a balance between PBB costs and the probability of not being able to service aircraft at contact gates. For each gate and time period it needs to be decided whether the PBB configuration from the previous time period should be retained or exchanged. Selecting a PBB configuration for a gate implies deciding on (a) the type(s) and (b) the number of bridges of the selected type(s) that are installed at the gate. Regarding (a), PBBs can be grouped into stationary and apron-drive bridges, see Figure 1. In contrast to stationary PBBs, apron-drive bridges are equipped with a rotatable connection to the terminal building and a drive column with wheel bogey. Consequently, they exhibit a higher operational flexibility but with the downside of higher investment and operational costs due to their greater technical complexity.

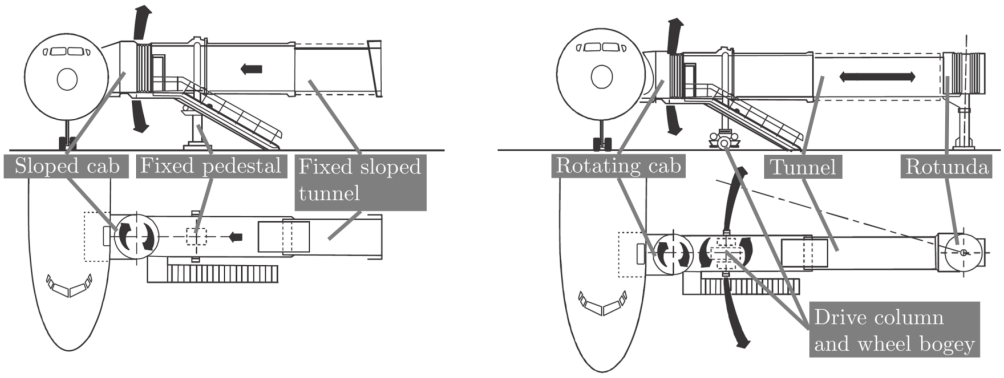

(a) Stationary loading bridge (b) Apron-drive loading bridge

Figure 1: Stationary and apron drive loading bridges (source: International Civil Aviation Organization 2005, edited according to Airport Cooperative Research Program 2010).

With respect to (b), either a single PBB or two PBBs of the same type are usually installed per gate. At gates that accommodate code F[3] aircraft, such as the Airbus A380, a third PBB is employed in order to expedite the boarding and deplaning operations. The aggregate of all PBB configurations represents all possible states of a gate with respect to PBBs, including the no-PBB case. The number of contact gates as well as the initial PBB configuration of each parking position are predefined, enabling both greenfield and brownfield scenarios to be modeled.

[3]according to International Civil Aviation Organization (2018)

In addition to the diverse PBB configurations, a multitude of commercial aircraft types exists, each with different specifications. As indicated by Kazda and Caves (2008), the variation in doorsill height across aircraft of different types causes incompatibilities between PBB configurations and aircraft types (also see Airport Cooperative Research Program 2010). In addition to these inevitable incompatibilities owing to aircraft and PBB geometries, it is not practical to serve certain types of aircraft with certain PBB configurations. For instance, there might be a PBB configuration that is defined as a single but flexible apron-drive PBB. Although this PBB might reach the doorsill of all aircraft on the market, boarding and deplaning operations would require an unacceptable duration for large types of aircraft. Consequently, the compatibility between PBB configurations and aircraft types is de facto restricted beyond the physical limitations, such that accommodation is physically possible *and* operations can be conducted with adequate efficiency. Due to the large variety of aircraft types and to account for aircraft that will be introduced to the market within the time horizon, we classify aircraft according to the commonly used wingspan criterion[4]. Consequently, we define the compatibilities between PBB configurations and aircraft classes rather than individual aircraft types. If a PBB configuration is compatible with a particular aircraft class, all aircraft of that class can be accommodated at a parking position equipped with that PBB configuration.

As we consider the problem in a dynamic context, we rely on forecasts that estimate the demand for accommodation for each aircraft class and time period in the time horizon. The decisions are taken at the beginning of each time period and configuration changes are realized instantly, such that any new configurations can be utilized in the respective time period. The following three cost types are relevant to the decision problem: First, a change in PBB configuration causes investment cost for dismantling and disposing the previous PBB configuration, gate unavailability during reconfiguration and the purchase and setup of the new PBB configuration. The actual amount depends on the PBB configurations before and after the change. For each period, we consider a constrained budget available to change PBB configurations. Second, installed PBB configurations cause operating costs over the course of the respective time period. These include the maintenance costs of the installed equipment (including vertical and horizontal drive motors, control systems and air-conditioning units) and thus depend on the PBB configuration. Third, in each time period, penalty costs are incurred for each aircraft that cannot be accommodated at one of the contact gates. Aircraft that cannot be processed at a contact gate need to be parked at a remote parking position and passengers then have to be conveyed from and to the aircraft by bus. On the one hand, this has a direct financial impact on the airport, as airlines pay fees for the use of PBBs at contact gates (for instance, see Aena 2020), which are, however, not incurred for aircraft processed at remote parking positions. On the other hand, this diminishes the operational efficiency at the airport, as it leads to longer connecting times for transfer passengers. Greater connection times reduce the hub potential of the affected airport as fewer connections can be offered within a given space of time. The penalty costs include the resulting costs accruing due to lost income, deteriorated

[4]Further criteria such as doorsill height, maximum number of passengers, and maximum takeoff weight are positively correlated with the wingspan measure, which is why a one-dimensional categorization is sufficient.

efficiency and lost connections, and the amount depends on the class of the relocated aircraft. The objective is to minimize the total cost, i.e., the sum of the investment, operating and penalty costs.

Demand patterns. Airlines and airports generally issue two flight plans per year, one for the summer and one for the winter season. As we have chosen a time period length of half a year, the length of a season matches the length of one time period, and each season is represented by one time period. Within each season, the flight schedules generally repeat in a weekly rhythm. Therefore, the flight traffic for each season can be represented by the flights observed in one representative week of that season. In the course of a week, the number of aircraft processed simultaneously is not constant but varies over time (Figure 7 in Section 7 shows an illustrative example of the number of aircraft processed simultaneously at Munich Airport Terminal 2 for a typical week).

We determine all the situations in one representative week where the total number of aircraft processed reaches a peak. Each situation is defined by the number of aircraft per class processed simultaneously and by a weighting factor. We denote the vector with the number of aircraft per class as the corresponding *demand pattern*. For example, a demand pattern $[3, 4, 5]$ states that 3, 4, and 5 aircraft of class 1, 2, and 3, respectively, are processed in parallel. The weighting factor is based on the relative frequency of the pattern. For example, if there are three different demand patterns which are observed with frequencies of 2, 3, and 1, respectively, the weights of the demand patterns are 0.33, 0.50, and 0.17, respectively.

The use of demand patterns has three major benefits. First, the amount of demand data is drastically reduced, while information relevant for demand fulfillment is retained. If the demand can be covered during all peak hours, a capacity shortage is unlikely to occur at other moments in time due to unavailable or incompatible PBBs. Second, estimating the number of aircraft and the fleet mix to be expected during peak hours is easier for airports to implement than forecasting the complete flight plan over the entire time horizon. Third, to account for forecasting uncertainty, the proposed approach allows the definition of several demand patterns, reflecting different possible future scenarios of one peak hour without any further changes being made to the concept.

Neighborhood restrictions. The accommodation of an aircraft at a gate might temporarily be prohibited due to potential wingtip collisions with other aircraft simultaneously parked at adjacent parking positions (Dorndorf, Jaehn, and Pesch 2017). This is relevant to our decision problem, as it induces restrictions to reasonable PBB configurations at the parking positions depending on the PBB configurations at the adjacent gates. For instance, there is no point in installing PBB configurations for large aircraft types at two adjacent gates if only one of the gates can serve one large aircraft at a time due to spatial restrictions. We consider a nose-in parking orientation of aircraft accommodated at contact gates as common at most airports (for further reference, see Horonjeff et al. 2010 and Kazda and Caves 2008). Gates comprise lead-in lines (see Airport Cooperative Research Program 2010), which guide aircraft from the taxiway on the apron to their final parking positions. The fuselages of parked aircraft are aligned with the lead-in lines. To

accommodate aircraft of different types and increase operational flexibility, a single parking position may have several lead-in lines.

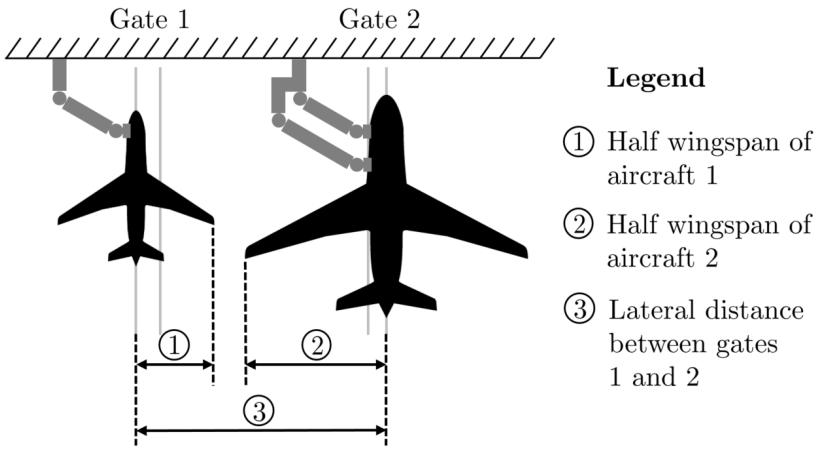

Figure 2: Lateral distance between adjacent gates and half wingspans

In order to prevent wingtip collisions of aircraft processed simultaneously at adjacent gates, the sum of the half wingspans of aircraft being processed on any combination of lead-in lines belonging to the gates must not exceed the lateral distance between the lead-in lines the aircraft are parked on. Consider the situation at the adjacent gates depicted in Figure 2, for example, where both gates are equipped with two parallel lead-in lines. As we have classified aircraft according to their wingspan, the wingspan of an aircraft is equal to the maximum wingspan of its aircraft class.

Multi Aircraft Ramping Stands. In order to enhance spatial efficiency, MARS gates have been introduced at many airports (see Airport Cooperative Research Program 2010). Up to two aircraft can be accommodated simultaneously at a MARS gate, depending on the size of the aircraft. To be able to process two smaller aircraft simultaneously, configurations of at least two PBBs have to be installed at MARS gates. Parking positions need to be equipped with at least three lead-in lines in order that they can be used as MARS gates. These include a central lead-in line for processing single aircraft and two outer lead-in lines to enable two aircraft to be accommodated simultaneously. Figure 3 presents the possible modes of operation of a MARS gate and illustrates the three parallel lead-in lines described.

For each PBB configuration, we define whether it can be employed at a MARS gate. While gates with no MARS-capable PBB configuration can only accommodate one aircraft at a time, the capacity restriction is two for gates with a MARS-capable PBB configuration. Furthermore, previous considerations of neighborhood restrictions need to be adapted to prevent wingtip collisions between two narrowbody aircraft parked simultaneously at a MARS gate. In addition to the existing constraints, which consider all combinations of lead-in lines at adjacent gates, it is now additionally necessary to check all combinations of lead-in lines individually for each single gate.

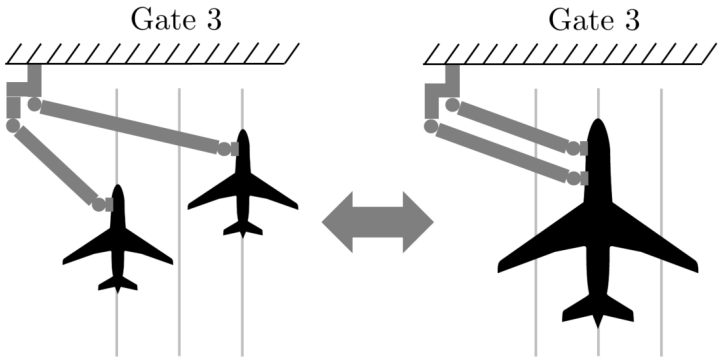

Figure 3: Modes of operation and lead-in lines of MARS gates

4 Model

In this section, we present a deterministic mathematical model for the dynamic gate configuration problem. A summary of the notation is given in Table 5 of Appendix A. As previously stated, the planning goal is to determine which PBB configuration should be installed at each gate, and when, in order to satisfy dynamic demands with minimum total cost. Planning is based on a discrete horizon $\mathcal{T} = \{0, \ldots, T\}$ with T time periods of equal length. The sets of gates and lead-in lines are denoted as $\mathcal{G} = \{0, \ldots, G\}$ and $\mathcal{J} = \{0, \ldots, J\}$, respectively. For each gate, disjoint sets $\mathcal{J}_g \subseteq \mathcal{J}$ contain the lead-in lines associated with gates $g \in \mathcal{G}$. At the beginning of each time period $t = \{0, \ldots, T-1\}$ it needs to be decided for each gate which PBB configuration of set $\mathcal{L} = \{0, \ldots, L\}$ should be installed, where $l = 0$ represents a dummy PBB configuration in which no PBB is installed at the respective gate. The set $\mathcal{L}^{MARS} \subseteq \mathcal{L}$ contains all PBB configurations which indicate that the respective gate is equipped as a MARS gate.

Time-space network. We model the problem as a time space network, in which each gate is represented by one subnetwork. The example in Figure 4 shows two gates, T periods and three PBB configurations.

The horizontal axis of each subnetwork constitutes the planning horizon, and the vertical axis the PBB configurations. Each node depicts a possible state of gate $g \in \mathcal{G}$ with respect to PBB configuration $l \in \mathcal{L}$ in time period $t \in \mathcal{T}$. The arcs represent feasible transitions from one node to another. The flow through arcs which connect nodes of different PBB configurations $k, l \in \mathcal{L}$ at the beginning of each period $t \in \mathcal{T}$ is determined by binary decision variables $x_{gtkl} \in \{0, 1\}$. Binary decision variables $z_{gtl} \in \{0, 1\}$ determine the flow through arcs connecting nodes that depict PBB configuration $l \in \mathcal{L}$ during period $t \in \mathcal{T}$. Variable x_{gtkl} is 1 if the construction of PBB configuration $l \in \mathcal{L}$ at gate $g \in \mathcal{G}$ is performed at the beginning of time period $t = 0, \ldots, T-1$ to substitute PBB configuration $k \in \mathcal{L} \setminus \{l\}$, and 0 otherwise. For the PBB configuration $l \in \mathcal{L}$ which is employed at gate $g \in \mathcal{G}$ during time period $t \in \mathcal{T}$, the respective variable z_{gtl} equals 1, and 0 otherwise. At

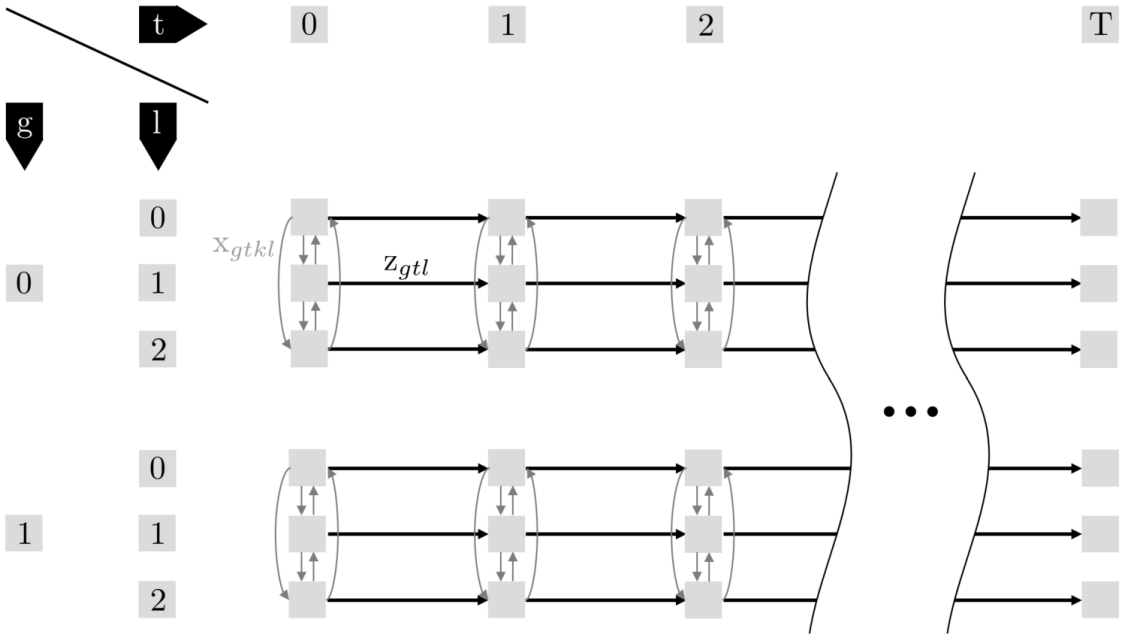

Figure 4: Time-space network

each node, a parameter e_{gtl} gives the difference between the sum of all inflows and the sum of all outflows. At the source node, i.e., the node at $t = 0$ representing the initial PBB configuration of the respective gate, inflows are 0 and outflows are 1 ($e_{gtl} = 1$). Furthermore, at each node in $t = 0, \ldots, T-1$ which is not a source of the network, the sum of all inflows must be equal to the sum of all outflows ($e_{gtl} = 0$) in order to ensure that the balance of flow is maintained.

Aircraft types and demand patterns. Aircraft are classified according to their wingspan, as stated in Section 3, and the resulting set of aircraft classes is denoted as $\mathcal{A} = \{1, \ldots, A\}$. For each aircraft class $a \in \mathcal{A}$, a set of PBB configurations that can be employed to accommodate aircraft of the respective class is introduced as $\mathcal{L}_a \subseteq \mathcal{L}$.

Future traffic volume is estimated by means of demand patterns as stated in Section 3. The demand patterns are enumerated in the set $\mathcal{B} = \{1, \ldots, B\}$. Parameter D_{ba} gives the number of aircraft of class $a \in \mathcal{A}$ in demand pattern $b \in \mathcal{B}$. Furthermore, for each time period $t \in \mathcal{T}$, the set $\mathcal{B}_t \subseteq \mathcal{B}$ contains the demand patterns of time period t. Weight f_{tb} gives the relative frequency of demand pattern $b \in \mathcal{B}_t$ in time period $t \in \mathcal{T}$. Since we assume that demand patterns and weights for the time horizon are given at the beginning of the decision process, our model is deterministic.

The degree to which demand (as represented by the demand patterns) can be fulfilled depends on the PBB configurations of the gates. Binary decision variable y_{gjtba} states if for demand pattern $b \in \mathcal{B}_t$ an aircraft of class $a \in \mathcal{A}$ is assigned to gate $g \in \mathcal{G}$ in time period $t \in \mathcal{T}$ using lead-in line $j \in \mathcal{J}_g$. Decision variables y^-_{tba} count the number of ungated aircraft. If for any demand pattern

$b \in \mathcal{B}_t$ in time period $t \in \mathcal{T}$ an aircraft of class $a \in \mathcal{A}$ cannot be accommodated at any of the contact gates, y^-_{tba} is increased by 1.

Aircraft at adjacent gates. For each parking position $g \in \mathcal{G}$, set $\mathcal{N}_g \subseteq \mathcal{G}$ is introduced, containing gate g and its right side neighbor gate $g+1$[5]. Further, the lateral distance between the lead-in lines $i \in \mathcal{J}$ and $j \in \mathcal{J}$ is denoted by the parameter d_{ij}. We define the parameter s_a as the lateral distance from the center of the fuselage to one of the wingtips (i.e. half the wingspan) of the aircraft with the largest wingspan in aircraft class $a \in \mathcal{A}$ plus an additional minimum separation distance, which must be adhered to. In the model, constraints will assure for each gate $g \in \mathcal{G}$ that for no combination of lead-in lines $i \in \mathcal{J}_h$ and $j \in \mathcal{J}_h$ ($i \neq j$ and $h \in \mathcal{N}_g$) does the sum of the adjusted aircraft wingspans s_a of the aircraft parked simultaneously at lead-in lines i and j exceed the value of d_{ij}. As lead-in lines i and j might be associated with the same gate, these constraints also cover the necessary neighborhood relations between two aircraft parked simultaneously at a MARS gate.

Costs and objective. The objective of minimizing the total cost implies minimizing the sum of three cost types. First, investment costs c^{i}_{kl} represent the costs of changing the PBB configuration at any gate for each combination ($k, l \in \mathcal{L}$) of unidentical PBB configurations. The total investment cost incurred in period $t \in \mathcal{T}$ is limited by the available budget r_t. Second, operating costs c^{o}_l measure the running costs for maintenance and of accommodating aircraft at an aircraft stand where PBB configuration $l \in \mathcal{L}$ is installed. Third, penalty costs c^- are incurred for each passenger who leaves or boards an aircraft parked at a remote position. In the objective function, c^- is multiplied by the parameter p_a, which gives the average number of passengers on board an aircraft of class $a \in \mathcal{A}$. Thus, the penalty cost incurred depends on the class of the respective aircraft which cannot be assigned to a contact gate.

Extensive formulation. We now present the extensive formulation of the passenger boarding bridge layout problem, which we denote as *Original Problem* OP.

$$\begin{aligned} \min\ z_{OP} \coloneqq & \sum_{g\in\mathcal{G}} \sum_{l\in\mathcal{L}} \sum_{k\in\mathcal{L}\setminus\{l\}} \sum_{t=0}^{T-1} c^{\mathrm{i}}_{kl} x_{gtkl} \\ & + \sum_{g\in\mathcal{G}} \sum_{t=0}^{T-1} \sum_{l\in\mathcal{L}} c^{\mathrm{o}}_l z_{gtl} \\ & + c^- \sum_{a\in\mathcal{A}} p_a \sum_{t=0}^{T-1} \sum_{b\in\mathcal{B}_t} f_{tb} y^-_{tba} \end{aligned} \tag{1a}$$

[5]The left side neighbor gate $g-1$ does not need to be considered as the combination of gates $g-1$ and g is already considered in the set $\mathcal{N}_{g-1}$.

subject to

$$\sum_{k\in\mathcal{L}\setminus\{l\}} x_{gtlk} + z_{gtl} \qquad \forall g \in \mathcal{G}, t = 0,\dots,T-1, \qquad (1b)$$

$$- \sum_{k\in\mathcal{L}\setminus\{l\}} x_{gtkl} - \sum_{\substack{t'=t:\\ t'>0}} z_{g,t'-1,l} = e_{gtl} \qquad l \in \mathcal{L}$$

$$\sum_{g\in\mathcal{G}} \sum_{j\in\mathcal{J}_g} y_{gjtba} + y^{-}_{tba} \geq D_{ba} \qquad \forall t = 0,\dots,T-1, \qquad (1c)$$

$$b \in \mathcal{B}_t, a \in \mathcal{A}$$

$$\sum_{g\in\mathcal{G}} \sum_{l\in\mathcal{L}} \sum_{k\in\mathcal{L}\setminus\{l\}} c^{\mathrm{i}}_{kl} x_{gtkl} \leq r_t \qquad \forall t = 0,\dots,T-1 \qquad (1d)$$

$$\sum_{a\in\mathcal{A}} y_{gjtba} \leq \sum_{l\in\mathcal{L}\setminus\{0\}} z_{gtl} \qquad \forall g \in \mathcal{G}, j \in \mathcal{J}_g, \qquad (1e)$$

$$t = 0,\dots,T-1, b \in \mathcal{B}_t$$

$$\sum_{a\in\mathcal{A}} \sum_{j\in\mathcal{J}_g} y_{gjtba} \leq 2 - \sum_{l\in\mathcal{L}\setminus\mathcal{L}^{MARS}} z_{gtl} \qquad \forall g \in \mathcal{G}, t = 0,\dots,T-1, \qquad (1f)$$

$$b \in \mathcal{B}_t$$

$$y_{gjtba} \leq \sum_{l\in\mathcal{L}_a} z_{gtl} \qquad \forall g \in \mathcal{G}, j \in \mathcal{J}_g, t = 0,\dots,T-1, \qquad (1g)$$

$$b \in \mathcal{B}_t, a \in \mathcal{A}$$

$$\sum_{a\in\mathcal{A}} y_{hitba} s_a + \sum_{a\in\mathcal{A}} y_{hjtba} s_a \leq \qquad \forall g \in \mathcal{G}, i, j \in \mathcal{J}_h : h \in \mathcal{N}_g, j > i, \qquad (1h)$$

$$d_{ij} + M \cdot \left(2 - \sum_{a\in\mathcal{A}} y_{hitba} - \sum_{a\in\mathcal{A}} y_{hjtba}\right) \qquad t = 0,\dots,T-1, b \in \mathcal{B}_t$$

$$x_{gtkl} \in \{0,1\} \qquad \forall g \in \mathcal{G}, k \in \mathcal{L}, l \in \mathcal{L}\setminus\{k\}, \qquad (1i)$$

$$t = 0,\dots,T-1$$

$$z_{gtl} \in \{0,1\} \qquad \forall g \in \mathcal{G}, t = 0,\dots,T-1, \qquad (1j)$$

$$l \in \mathcal{L}$$

$$y^{-}_{tba} \geq 0 \qquad \forall t = 0,\dots,T-1, \qquad (1k)$$

$$b \in \mathcal{B}_t, a \in \mathcal{A}$$

$$y_{gjtba} \in \{0,1\} \qquad \forall g \in \mathcal{G}, j \in \mathcal{J}_g, t = 0,\dots,T-1, \qquad (1l)$$

$$b \in \mathcal{B}_t, a \in \mathcal{A}$$

Objective function (1a) minimizes the sum of the investment, operating and penalty costs. Constraints (1b) are the flow balance equations and constraints (1c) require that demands are satisfied, otherwise a penalty is incurred. Budget constraints (1d) make sure that the budget available for PBB configuration changes is not exceeded in any time period. Capacity constraints (1e) ensure that no aircraft can be assigned to a lead-in line which belongs to a gate that does

not have any PBB installed. Additional capacity constraints (1f) ensure that at gates which are not equipped with a MARS-capable PBB configuration, no more than one aircraft can be serviced simultaneously, while at gates where a MARS-capable PBB configuration is installed, at most two aircraft can be accommodated at a time. Constraints (1g) ensure that only aircraft stands with compatible PBB configurations are used to serve the demands of each aircraft class. Neighborhood constraints (1h) ensure that restrictions on aircraft parking simultaneously at adjacent gates and MARS gates are adhered to. We set the value of the Big-M parameter used in these constraints to $\max_{a\in\mathcal{A}} s_a$. Finally, constraints (1i) – (1l) define the variable domains.

5 Solution Methodology

In the computational study that follows in Section 6, it will be seen that OP (1a)-(1l) is too large to be solvable within a reasonable amount of time for data instances of realistic size. When ignoring the gate assignment variables y^-_{tba} and y_{gjtba}, the penalty costs in objective function (1a) and related constraints (1c)-(1h), OP can be reduced to a multi-commodity flow problem, where for each gate $g \in \mathcal{G}$ a shortest path problem has to be solved (see Figure (4)). Due to this natural decomposition of the problem, we suggest to reformulate OP by applying Dantzig-Wolfe decomposition and to solve the reformulated model using a column generation (CG) heuristic. Desrosiers and Lübbecke (2005) show that the extreme points of the polyhedron defined by a shortest path problem correspond to paths through the flow network. In our case, the flow network is the one presented in Figure (4) and a *path* is defined as a sequence of nodes leading from the source to the sink of the graph associated with one gate. A path thus defines the PBB configuration of one gate for each time period within the time horizon. In addition to the notation presented in Table 5, the terminology provided in Table 6 will be used in the following. All paths (of all gates) are contained in the set $\mathcal{P} = \{1, \ldots, P\}$, and for each gate $g \in \mathcal{G}$, a set $\mathcal{P}_g \subseteq \mathcal{P}$ contains all paths associated with the respective gate. Furthermore, each path is associated with path cost c_p, which equals the sum of investment and operating costs accumulated through the respective path. Instead of deciding for each gate and time period whether the current PBB configuration should be retained or replaced by a different one by setting binary decision variables x_{gtkl} and z_{gtl}, the decision now is whether or not to select path $p \in \mathcal{P}_g$ for gate $g \in \mathcal{G}$, represented by binary decision variables λ_p. Binary parameters z^p_{gtl} indicate whether or not gate $g \in \mathcal{G}$ is equipped with PBB configuration $l \in \mathcal{L}$ in time period $t \in \mathcal{T}$ and path $p \in \mathcal{P}_g$. Similarly, binary parameters x^p_{gtkl} indicate whether or not the PBB configuration $l \in \mathcal{L}$ is replaced by PBB configuration $k \in \mathcal{L}$ at gate $g \in \mathcal{G}$ in time period $t \in \mathcal{T}$.

Master Problem. Given our definition of a path and the presented notation, reformulation of OP yields the following *Master Problem* MP:

$$\min\ z_{MP} \coloneqq \sum_{p\in\mathcal{P}} c_p\lambda_p + c^- \sum_{a\in\mathcal{A}} p_a \sum_{t=0}^{T-1} \sum_{b\in\mathcal{B}_t} f_{tb} y^-_{tba} \tag{2a}$$

subject to

$$\sum_{g\in\mathcal{G}} \sum_{j\in\mathcal{J}_g} y_{gjtba} + y^-_{tba} \geq D_{ba} \qquad \forall t = 0,\dots,T-1,\ b\in\mathcal{B}_t, a\in\mathcal{A} \tag{2b}$$

$$\sum_{g\in\mathcal{G}} \sum_{p\in\mathcal{P}_g} \lambda_p \left(\sum_{l\in\mathcal{L}} \sum_{k\in\mathcal{L}\setminus\{l\}} c^{\mathrm{i}}_{kl} x_{gtkl} \right) \leq r_t \qquad \forall t = 0,\dots,T-1 \tag{2c}$$

$$\sum_{a\in\mathcal{A}} y_{gjtba} \leq \sum_{p\in\mathcal{P}_g} \lambda_p \left(\sum_{l\in\mathcal{L}\setminus\{0\}} z^p_{gtl} \right) \qquad \forall g\in\mathcal{G}, j\in\mathcal{J}_g,\ t=0,\dots,T-1, b\in\mathcal{B}_t \tag{2d}$$

$$\sum_{a\in\mathcal{A}} \sum_{j\in\mathcal{J}_g} y_{gjtba} \leq 2 - \sum_{p\in\mathcal{P}_g} \lambda_p \left(\sum_{l\in\mathcal{L}\setminus\mathcal{L}^{MARS}} z^p_{gtl} \right) \qquad \forall g\in\mathcal{G}, t=0,\dots,T-1,\ b\in\mathcal{B}_t \tag{2e}$$

$$y_{gjtba} \leq \sum_{p\in\mathcal{P}_g} \lambda_p \left(\sum_{l\in\mathcal{L}_a} z^p_{gtl} \right) \qquad \forall g\in\mathcal{G}, j\in\mathcal{J}_g, t=0,\dots,T-1,\ b\in\mathcal{B}_t, a\in\mathcal{A} \tag{2f}$$

$$\sum_{a\in\mathcal{A}} y_{hitba} s_a + \sum_{a\in\mathcal{A}} y_{hjtba} s_a \leq d_{ij} + M\cdot\left(2 - \sum_{a\in\mathcal{A}} y_{hitba} - \sum_{a\in\mathcal{A}} y_{hjtba}\right) \qquad \forall g\in\mathcal{G}, i,j\in\mathcal{J}_h : h\in\mathcal{N}_g, j>i,\ t=0,\dots,T-1, b\in\mathcal{B}_t \tag{2g}$$

$$\sum_{p\in\mathcal{P}_g} \lambda_p = 1 \qquad \forall g\in\mathcal{G} \tag{2h}$$

$$y^-_{tba} \geq 0 \qquad \forall t=0,\dots,T-1, b\in\mathcal{B}_t, a\in\mathcal{A} \tag{2i}$$

$$y_{gjtba} \in \{0,1\} \qquad \forall g\in\mathcal{G}, j\in\mathcal{J}_g, t=0,\dots,T-1,\ b\in\mathcal{B}_t, a\in\mathcal{A} \tag{2j}$$

$$\lambda_p \in \{0,1\} \qquad \forall p\in\mathcal{P} \tag{2k}$$

Note that the flow balance constraint is incorporated in the definition of a path and is therefore not represented in MP. The same holds for constraints (1i) and (1j), because decision variables

x_{gtkl} and z_{gtl} have been replaced and z^p_{gtl} and x^p_{gtkl} are now parameters. Constraints (1d), (1e), (1f) and (1g) are modified to (2c), (2d), (2e) and (2f) according to the altered notation, and convexity constraints (2h) need to be added as one path per gate needs to be selected.

Column Generation. For practical data instances, $\mathcal{P}$ will be prohibitively large. Explicitly enumerating and evaluating all possible paths in MP therefore becomes intractable. Hence, we derive the *Restricted Master Problem* RMP from MP by substituting $\mathcal{P}$ with the subset of paths $\mathcal{P}' \subseteq \mathcal{P}$. In order to apply the CG approach, we relax the integrality requirements on decision variables λ_p and y_{gjtba} and denote the resulting, relaxed version of RMP as $\widetilde{\text{RMP}}$. Similarly, the version of MP where integrality requirements on decision variables λ_p and y_{gjtba} are relaxed is referred to as $\widetilde{\text{MP}}$. After the initialization of $\widetilde{\text{RMP}}$ with a dummy path for each aircraft stand $g \in \mathcal{G}$, the CG procedure is commenced by solving $\widetilde{\text{RMP}}$ to optimality. Then, the dual variable values of constraints 2c, (2d), (2e), (2f) and (2h) are used to determine whether for any aircraft stand a new path can be found with negative reduced cost. This is done by solving G subproblems - one for each gate $g \in \mathcal{G}$. If for any gate(s) a path with negative reduced cost can be found, the latter is/are added to $\widetilde{\text{RMP}}$ and the process is repeated until no path with negative reduced cost can be found. The resulting solution is optimal to $\widetilde{\text{MP}}$ and the CG process is terminated.

A CG approach has to define how many subproblems should be solved after each re-optimization of $\widetilde{\text{RMP}}$ and how many of the found columns should be added to $\widetilde{\text{RMP}}$ in each iteration (see Morabit, Desaulniers, and Lodi 2020, , for instance). While adding only one column per iteration may lead to a large number of (potentially expensive) $\widetilde{\text{RMP}}$ re-optimizations, columns which are added to $\widetilde{\text{RMP}}$ in the same iteration are derived from the same dual variable values and thus are likely to be very similar, possibly inducing undesired symmetries to the problem. We opt for a balanced approach, which considers both aspects, in which, before launching the CG procedure, the gates are assigned to groups of size ≥ 1. In each iteration, the subproblems associated with one group are solved to optimality and the columns that are found (at most one per gate) are added to $\widetilde{\text{RMP}}$. The gates are allocated to the groups, such that the lateral distances between the gates of one group are maximized. The aim is to mitigate the effect of adding columns responding to the same dual variable values.

Subproblems. Let π^{bud}_t, $\pi^{\text{cap,line}}_{jtb}$, $\pi^{\text{cap,gate}}_{tb}$, π^{com}_{jtba} and π^{con} denote the dual variable values of constraints 2c, (2d), (2e), (2f) and (2h) associated with aircraft stand $g \in \mathcal{G}$, respectively. Then, for this gate the reduced cost of the best path which could be added to $\widetilde{\text{RMP}}$ is calculated by solving the following *Subproblem* SP to optimality:

$$\min\ \bar{c}^g \coloneqq \sum_{l\in\mathcal{L}}\sum_{k\in\mathcal{L}\setminus\{l\}}\sum_{t=0}^{T-1} c^{\mathrm{i}}_{kl}\left(1-\pi^{\mathrm{bud}}_t\right)x_{tkl} \tag{3a}$$
$$+\sum_{t=0}^{T-1}\sum_{l\in\mathcal{L}}\Bigg(c^{\mathrm{o}}_l+\sum_{j\in\mathcal{J}_g}\sum_{b\in\mathcal{B}_t}\sum_{\substack{l'\in\mathcal{L}\setminus\{0\}:\\ l'=l}}\pi^{\mathrm{cap,line}}_{jtb}$$
$$-\sum_{b\in\mathcal{B}_t}\sum_{\substack{l'\in\mathcal{L}\setminus\mathcal{L}^{MARS}:\\ l'=l}}\pi^{\mathrm{cap,gate}}_{tb}$$
$$+\sum_{j\in\mathcal{J}_g}\sum_{b\in\mathcal{B}_t}\sum_{a\in A}\sum_{\substack{l'\in\mathcal{L}_a:\\ l'=l}}\pi^{\mathrm{com}}_{jtba}\Bigg)z_{tl}-\pi^{\mathrm{con}}$$

subject to

$$\sum_{k\in\mathcal{L}\setminus\{l\}}x_{tlk}+z_{tl} \qquad \forall t=0,\dots,T-1, l\in\mathcal{L} \tag{3b}$$
$$-\sum_{k\in\mathcal{L}\setminus\{l\}}x_{t'kl}-\sum_{\substack{t'=t:\\ t'>0}}z_{t'-1,l}=e_{tl}$$
$$x_{tkl}\in\{0,1\} \qquad \forall k\in\mathcal{L}, l\in\mathcal{L}\setminus\{k\}, \tag{3c}$$
$$t=0,\dots,T-1$$
$$z_{tl}\in\{0,1\} \qquad \forall t=0,\dots,T-1, l\in\mathcal{L} \tag{3d}$$

The index g is removed from all parameters and variables, as SP is solved for each aircraft stand $g\in\mathcal{G}$ individually. We solve the subproblems efficiently by means of dynamic programming. That is, we find the shortest path through the (sub-)network corresponding to the respective gate as shown in Figure 4. The initial PBB configuration of the gate in $t=0$ constitutes the source of the network, and in $t=T+1$, we add a supersink which is connected with each node of $t=T$. The weight w_{klt} of the arc connecting the node representing PBB configuration $k\in\mathcal{L}$ in time period $t\in\mathcal{T}$ with the node depicting PBB configuration $l\in\mathcal{L}$ in time period $(t+1)\in\mathcal{T}$ is calculated as

$$w_{klt}=c^{\mathrm{o}}_l+c^{\mathrm{i}}_{kl}\left(1-\pi^{\mathrm{bud}}_t\right)+\sum_{j\in\mathcal{J}_g}\sum_{b\in\mathcal{B}_t}\sum_{\substack{l'\in\mathcal{L}\setminus\{0\}:\\ l'=l}}\pi^{\mathrm{cap,line}}_{jtb}-\sum_{b\in\mathcal{B}_t}\sum_{\substack{l'\in\mathcal{L}\setminus\mathcal{L}^{MARS}:\\ l'=l}}\pi^{\mathrm{cap,gate}}_{tb}+\sum_{j\in\mathcal{J}_g}\sum_{b\in\mathcal{B}_t}\sum_{a\in A}\sum_{\substack{l'\in\mathcal{L}_a:\\ l'=l}}\pi^{\mathrm{com}}_{jtba}.$$

If $k=l$ the term $c^{\mathrm{i}}_{kl}\left(1-\pi^{\mathrm{bud}}_t\right)$ is omitted. The weight of the arcs connecting the nodes of $t=T$ with the supersink is set to 0.

Obtaining integral solutions. Solving $\widetilde{\text{RMP}}$ gives us an optimal solution to $\widetilde{\text{MP}}$, but this may not necessarily be an integral solution. We therefore employ the following heuristic approach to obtain an integral solution to OP. As soon as the CG process is terminated, the integrality constraints on decision variables λ_p and y_{gjtba} are restored in $\widetilde{\text{RMP}}$ and the resulting RMP$'$ is solved by a commercial solver. This approach is a heuristic, as only the paths added to $\widetilde{\text{RMP}}$ during the CG procedure can be used in the optimal solution to RMP$'$. Furthermore, to counteract the slow convergence behavior of RMP$'$ when close to the optimal solution, we abort the optimization process of RMP$'$ when the duality gap reaches a sufficiently small value. The solution approach is illustrated as pseudo-code in Algorithm 1. The computational study will show that this allows us to find integral solutions of a given quality more quickly than the commercial solver when solving OP (1a)-(1l).

Algorithm 1 Proposed CG heursitic

```
START
Initialize RMP~ and one SP per gate, create N gate groups
columnFound := true
n := 0
WHILE columnFound = true DO
    Solve RMP~ and get dual variable values
    columnFound := false
    IF n = N + 1 THEN
        n := 0
    ENDIF
    FOR all gates belonging to group n
        Solve SP with the dual variable values from RMP~
        c := objective function value of SP
        IF c ≤ 0 THEN
            Add the respective column to RMP~
            columnFound := true
        ENDIF
    ENDFOR
    n := n + 1
    IF columnFound = false THEN
        FOR all gates
            Solve SP with the dual variable values from RMP~
            c := objective function value of SP
            IF c ≤ 0 THEN
              Add the respective column to RMP~
              columnFound := true
            ENDIF
        ENDFOR
    ENDIF
ENDWHILE
Add integrality constraints to the path variables of RMP~ to obtain RMP
Solve RMP until the desired duality gap is reached
Return the obtained solution
END
```

6 Computational Study

The numerical analysis presented in this section investigates the computational performance of the proposed CG heuristic and consists of four parts. First, we introduce how the data instances used in the following experiments were generated. Second, we investigate the performance obtained when solving OP (1a)-(1l) to optimality using a commercial solver. Third, we vary the parameters of the proposed CG heuristic to find a good setting with respect to both solution quality and runtime. Finally, we demonstrate the effectiveness of the CG heuristic by comparing its performance to solving OP. All experiments were conducted on a computer equipped with an octa-core CPU running at 3.8GHz and 32GB of RAM, while Gurobi 9.1 was employed as a commercial solver. The algorithms were implemented in Java, using the Gurobi API.

6.1 Generation of data instances

To investigate the performance of the solution methods, we generated problem instances of different sizes. We model an airport terminal with $G \in \{10, 15, 20\}$ contact gates, each gate being equipped with four lead-in lines, thus $J = 4 \cdot G$. The length of the time horizon is $T \in \{10, 15, 20\}$. The number of aircraft types is set to $A = 3$ (small, medium, large aircraft with maximum half wingspans s_a of 20, 34, and 44 meters, respectively). There are $L = 5$ PBB configurations available, where $l = 0$ denotes the "no PBB" case and $l = 4$ represents a MARS PBB configuration. The compatibilies between aircraft classes and PBB configurations are defined as $\mathcal{L}_1 = \{1, 2, 3, 4\}$, $\mathcal{L}_2 = \{2, 3, 4\}$, and $\mathcal{L}_3 = \{3, 4\}$. Figure 5 shows the five configurations employed in the computational study, including the "no PBB" case (configuration 0).

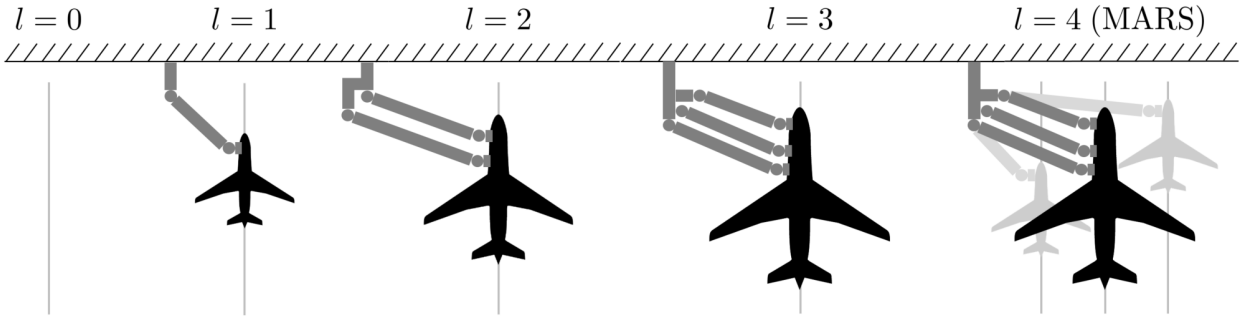

Figure 5: PBB configurations in the computational study

At $t = 0$, all gates have PBB configuration $l = 1$ installed and the distance between each pair of adjacent aircraft stands is set to 60 meters. Each gate is equipped with two inner lead-in lines located five meters to the left and right of the center of the gate, respectively. To allow for MARS operations, each aircraft stand is additionally equipped with two outer lead-in lines, which are placed 25 meters left and right from the center line of the gate, respectively. Since we cannot disclose real cost data, we use the following cost factors reflecting the relationship between the

different costs: $c^{\mathrm{i}}_{kl} = \begin{pmatrix} 0 & 8 & 16 & 24 & 32 \\ 8 & 0 & 8 & 16 & 24 \\ 8 & 8 & 0 & 8 & 16 \\ 8 & 8 & 8 & 0 & 16 \\ 8 & 8 & 8 & 8 & 0 \end{pmatrix}$, $c^{\mathrm{o}}_{l} = (\ 0.5 \quad 1.5 \quad 2.5 \quad 3.5 \quad 4.5\ )$ and $c^{-} = 0.02$. The more flexible a PBB configuration l is, the higher are its investment costs c^{i}_{kl} and operating cost c^{o}_{l}. As for the value of c^{-}, the case study presented in Section 7 will demonstrate that 0.02 is a reasonable value for a quality oriented airport with respect to the given values of c^{i}_{kl} and c^{o}_{l}. The aircraft classes are weighted with $p_a = (\ 150 \quad 300 \quad 400\ )$, approximately corresponding with the number of passengers carried by the respective types of aircraft. While we investigate the impact of different values of r on the solution in the case study in Section (7), we relax budget constraints (1d) and (2c) within the scope of the computational study in this section. Regarding the development of air traffic over the time horizon, we model a scenario where a high traffic volume (i.e., approximately G aircraft per demand pattern) throughout the time horizon is combined with a shift in the fleet mix towards larger aircraft. In recent decades, this scenario was frequently observed at airports where the construction of additional capacities (runways, terminals, etc.) was not possible in the medium term although passenger volume was increasing (London Heathrow, for instance).

For each combination of G and T we generated 20 instances, which gives $3 \cdot 3 \cdot 20 = 180$ instances in total. In the following, we will refer to the instances of one G and T as *instance class*. The 20 instances of one instance class differ with respect to the demand patterns as well as the relative weighting of the patterns:

- The demand patterns in $\mathcal{B}_t$ are selected randomly from a predefined set of demand patterns $\mathcal{B}$ for each time period $t \in \mathcal{T}$, such that three demand patterns are allocated to each time period and the described development of air traffic over the time horizon is replicated[6].
- The weighting factors f_{tb} take random values between $]0;1[$, where for each time period $\sum_{b \in \mathcal{B}_t} f_{tb} = 1$ must hold.

We divided the 180 instances into two batches of 90 instances each, where each batch contains 10 instances of each instance class.

6.2 Solving OP to optimality using a commercial solver

We applied the commercial solver to the first batch of instances. Table 1 presents the average computation times of OP for each instance class.

[6]Further details are provided in Appendix B.

Table 1: Average computation times of OP (1a)-(1l) [min]

	$T = 10$	$T = 15$	$T = 20$
$G = 10$	1.78	5.00	23.81
$G = 15$	13.59	61.07	129.29
$G = 20$	24.38	94.29	674.54[7]

Computation times increase considerably when the values of T and G are increased. It is apparent that the commercial solver cannot efficiently solve OP to optimality for larger instances. We observe three instances where $T = G = 20$, for which the solution process is not completed within 24 hours. OP is thus not applicable to data instances of realistic size where G and T may both take values larger than 20 (e.g., Munich airport has $G = 58$ contact gates[8]) and the number of demand patterns for each time period might be larger than three.

6.3 Approximating optimal solutions using the CG heuristic

When applying the CG heuristic, the following parameters have to be set:

- The number of gates per group as defined for the iterative optimization process of $\widetilde{\text{RMP}}$, denoted as *group_size*.
- The duality gap that needs to be reached to abort the optimization process of RMP$'$, denoted as *rmp_gap*.

We tested the computational performance of the CG heuristic for all combinations of *group_size* $\in \{1, 2, 4, 10\}$ and *rmp_gap* $\in \{0, 2.5\%, 5\%, 10\%, 12.5\%, 15\%, 17.5\%, 20\%\}$. Thus, we applied the heuristic $4 \cdot 8 = 32$ times to each of the 90 data instances of the first batch.

To find the best values for *group_size* and *rmp_gap*, we investigated the performance of each value combination of these parameters for every instance class. More precisely, we calculated for each instance class and value combination of *group_size* and *rmp_gap* (a) the average percentage deviation from the optimum (referred to as *optimality gap*) and (b) the average total runtime[9]. We normalized the values of both (a) and (b) to be in $[0; 1]$ by $v^n = \frac{v - v^{min}}{v^{max} - v^{min}}$, where normalized values close to zero indicate small optimality gaps for (a) and short runtimes for (b)[10]. In the following, we will refer to the normalized values as *quality* and *runtime scores*, respectively. Figures 6a and 6b provide the average quality and runtime scores of each parmeter combination over all instance classes.

As expected, the setting of both *group_size* and *rmp_gap* parameters has a clear impact on the performance of the CG heuristic. Increasing *rmp_gap* leads to a worsening of the quality

[7] The optimization process of three instances was aborted after 24 hours.

[8] as of January 2020

[9] The optimum objective function values were obtained by solving OP with unlimited runtime.

[10] For *group_size* $= 10$ and *rmp_gap* $= 0$ we found considerably higher runtimes for all instance classes compared to other parameter combinations. In order to obtain reasonable values by the normalization, we excluded this parameter combination from the normalization procedure and set its value to 1 for all instance classes.

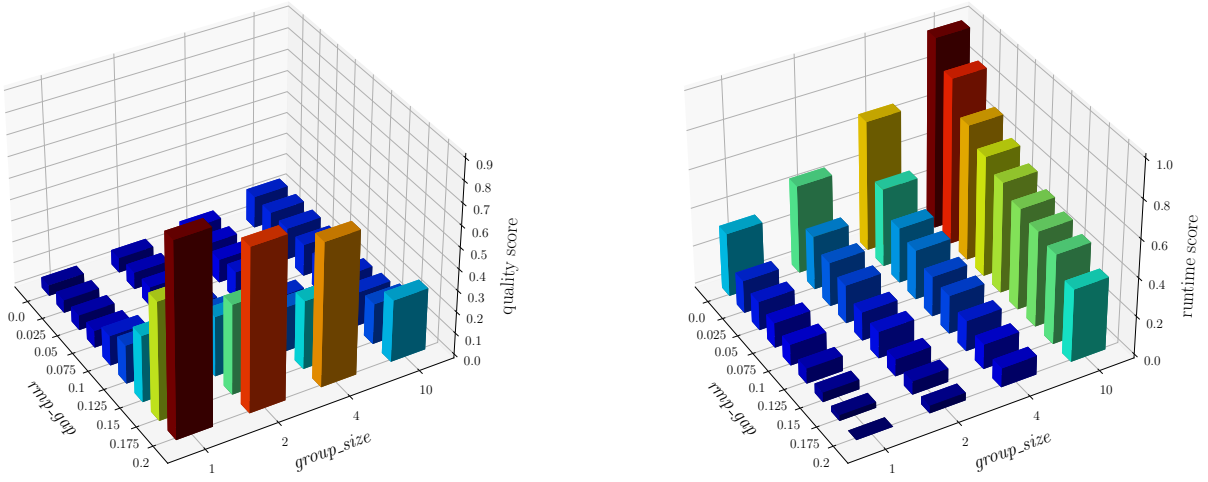

(a) Average quality scores for different parameter combinations

(b) Average runtime scores for different parameter combinations

Figure 6

score (i.e., an increase in the optimality gaps) and an improvement of the runtime score (i.e., shorter computation times). We find that the value of *group_size* only has a notable impact on the quality score for large values of *rmp_gap*. However, the best quality scores are observed when $group\_size = 1$ and *rmp_gap* is small. With respect to the runtime score, *group_size* has a larger impact when the value of *rmp_gap* is small. Again, the best runtime scores were observed for $group\_size = 1$. We conclude that the disadvantage of solving fewer subproblems per iteration (potentially resulting in many necessary $\widetilde{\text{RMP}}$ re-optimization cycles, see Section 5) is smaller than the negative effect of adding multiple similar columns to $\widetilde{\text{RMP}}$ per iteration (which results from larger values of *group_size*) in our case.

As small optimality gaps and short runtimes are conflicting goals, there is no dominating parameter setting. For the following experiments, we selected the parameter combination with the smallest sum of quality and runtime scores, as shown in Figures 6a and 6b. This is the case for $group\_size = 1$ and $rmp\_gap = 0.075$. With these parameter values, the final heuristic solution is found after 2.15 minutes and the optimality gap is 1.99%, averaged over all instance classes.

6.4 Validating the performance of the CG heuristic

To validate the performance of the CG heuristic with the given parameter values, we applied it to the second batch of instances created in Subsection (6.1).

Tables 2a-2c present the results when applying the CG heuristic with the parameters as selected in Subsection 6.3 to these instances. As a valid benchmark for the computation times of the CG heuristic, we solved each instance with OP (1a)-(1l) and aborted the solution procedure once the objective function value obtained by the CG heuristic was reached. Furthermore, we solved OP to

optimality as presented in Subsection 6.2 in order to calculate the optimality gaps.

	$T = 10$	$T = 15$	$T = 20$
$G = 10$	0.24	0.92	2.10
$G = 15$	0.35	1.52	3.61
$G = 20$	0.60	2.35	6.29

(a) Average computation times of CG heuristic [min]

	$T = 10$	$T = 15$	$T = 20$
$G = 10$	0.87	1.18	0.87
$G = 15$	0.46	0.51	0.57
$G = 20$	0.62	0.86	0.62

(b) Average computation times of CG heuristic divided by average computation times of OP with abortion criterion

	$T = 10$	$T = 15$	$T = 20$
$G = 10$	1.96	2.68	2.35
$G = 15$	1.54	1.18	2.29
$G = 20$	2.20	1.93	1.95

(c) Average optimality gaps of CG heuristic [%]

Table 2

The results demonstrate the efficiency of the proposed CG heuristic. With optimality gaps between 1.18% and 2.68%, the CG heuristic reaches its final objective function value on average in less than 73% of the runtime needed by the commercial solver to find a solution of equal quality. With the exception of one relatively small instance class ($G = 10$ and $T = 15$), where the commercial solver finds the final objective function value provided by the CG heuristic faster than the CG heuristic and where the optimality gap reaches its maximum, the CG heuristic thoroughly outperforms the commercial solver.

7 Case Study

In the case study, we consider the current situation at Munich Airport Terminal 2. For our analysis, we modeled the contact gates of the terminal, generated demand patterns based on real traffic data, and considered the current crisis caused by the SARS-CoV-2 virus[11]. We provide the data set containing all information that is needed to reproduce the case study in Hagspihl et al. (2021). In the following two subsections 7.1 and 7.2, we investigate the impact of different values of penalty cost c^- and the available budget per period r on the solution proposed by the CG heuristic.

Munich Airport is a major European hub airport with a passenger volume of 48.0 million in 2019 (Munich Airport 2020). Passengers are processed via two terminals, where Terminal 2 including its satellite building is the high-quality hub terminal used by member airlines of the Star Alliance and provides approximately double the capacity of Terminal 1. Terminal 2 possesses $G = 47$ contact gates, each of which is equipped with one to three lead-in lines. The contact gates are equipped with apron-drive PBBs, where up to three bridges are installed per gate. Currently four gates are in use as MARS gates.

[11] We do not need to consider the entire airport, as Terminal 2 is used exclusively by member airlines of the Star Alliance and thus the traffic can be forecast individually for this part of the airport.

Along the lines of the computational study, we considered $L = 5$ PBB configurations (0: No PBB; 1: Single apron-drive PBB; 2: Two apron-drive PBBs; 3: Three apron-drive PBBs; 4: MARS) and $A = 3$ aircraft classes with maximum half wingspans s_a of 20, 34 and 44 meters, respectively. The compatibilities between PBB configurations and aircraft classes were defined as in Section 6.1, and we set the length of the time horizon to $T = 20$ time periods, representing the time span from summer 2019 to summer 2029.

As for the development of demand over time, we modeled the current situation, which is heavily impacted by the SARS-CoV-2 virus. That is, we modeled an abrupt but temporary drop in air traffic volume in 2020, followed by a continual recovery from the low point reached. To generate the demand patterns, we analyzed a representative week of the flight plan of Munich Airport for the summer period of 2019. Of all flights listed for that week, we only considered those that were processed at a gate (contact or remote) belonging to Terminal 2. Using the list of the relevant arrivals and departures, we calculated the number of aircraft which were simultaneously accommodated on the apron of Terminal 2, with a time granularity of five minutes. Figure 7 presents the resulting number of aircraft at a gate over time, which demonstrates the aforementioned oscillatory behavior.

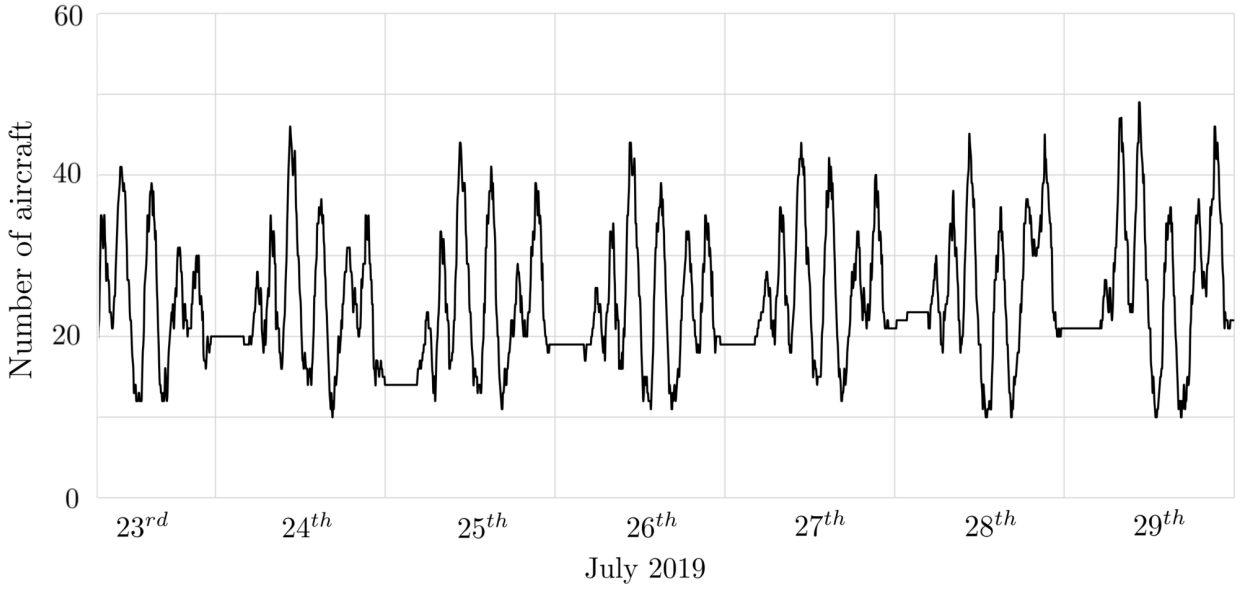

Figure 7: Number of aircraft accommodated simultaneously at Munich Airport Terminal 2 over one typical week in summer 2019

To derive the relevant demand patterns, we first determined the number of aircraft of each class to be accommodated simultaneously for each peak. We then identified those demand patterns that are not dominated by others[12]. This procedure revealed four demand patterns to be included in the model for the period of summer 2019. This enabled us to generate demand patterns for the

[12] A pattern $b = 1$ dominates another pattern $b = 2$ if for all $a \in \mathcal{A}$ the term $D_{1a} \geq D_{2a}$ holds and for at least one $a \in \mathcal{A}$ the inequality $D_{1a} > D_{2a}$ is satisfied.

following time periods, such that $\mid \mathcal{B}_t \mid = 4$ for each $t \in \mathcal{T}$. More specifically, the demand patterns for $t \in \{1, 2, 10, 19\}$ were generated as follows. In periods 1 and 2, the patterns follow the steep decrease in traffic caused by the SARS-CoV-2 crisis. The demand patterns of $t = 10$ equal those of period 0, based on the assumption that the demand will have recovered from the crisis by then. The demand patterns of the last period $t = 19$ are based on those of $t = 10$, ensuring that the demand is stationary with low variance after $t = 10$; however, based on recent developments around the Airbus A380 and the Boeing 747, the largest class of aircraft becomes less frequent. For $t \in [3, 9]$, the demand patterns were interpolated between the patterns of $t = 2$ and $t = 10$, and random but seasonally biased deviations were added[13]. For $t \in [11, 18]$, the same method was applied using the patterns of $t = 10$ and $t = 19$ for the interpolation. Figure 8 shows the number of aircraft of each class over the time horizon, averaged for the demand patterns over the respective time period.

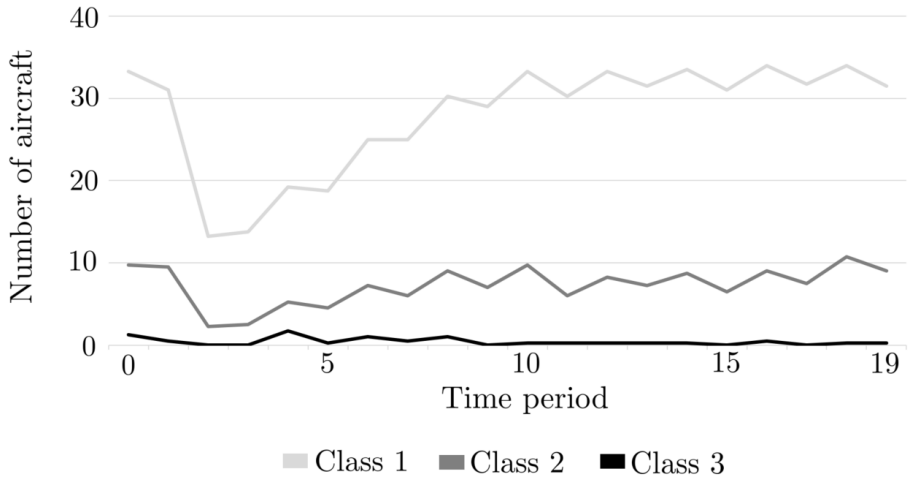

Figure 8: Average number of aircraft of each class as represented in the demand patterns over the time horizon

7.1 Investigating the impact of different penalty cost values

In practice, both the costs c^{i}_{kl}, c^{o}_{l}, and the aircraft class weights p_a are given exogeneously by PBB and aircraft manufacturers. In contrast, the penalty cost c^{-} depends on the desired service quality the airport aims to offer to its customers: Accommodating an aircraft at a remote parking position leads to a higher penalty cost at a quality oriented hub airport than at a low cost oriented small airport. For the following analysis, we set c^{i}_{kl}, c^{o}_{l} and p_a to the values given in Section 6.1, whereas we varied the value of c^{-} within $[0; 0.3]$ with a step size of 0.005, which allows us to analyze the effect of service quality on the decisions taken and the different cost components. While we investigate the impact of different budgets in Subsection 7.2, the investigation of different penalty

[13] A random value was added to each value of D_{ba}. If pattern $b \in \mathcal{B}$ is associated with a winter period, the value was chosen from $[-3, -1]$, otherwise from $[1, 3]$.

cost values is based on relaxed budget constraints (2c), which is also in line with Subsection 6.1. For simplicity reasons, all weights f_{tb} were set to 0.25.

Averaged over all values of c^-, the CG heuristic with $group\_size = 1$ and $rmp\_gap = 0.075$ solves the instance in 2.83 minutes. The objective function value (the total cost) obtained by the CG heuristic is 1612.35 on average. When solving the CG heuristic with the additional constraint that the PBB configurations installed in summer 2019 must not be changed, the objective function value is 2006.88 on average. Consequently, averaged over all values of c^- and under the assumption that the future traffic development represented by the demand patterns indeed materializes in the future, changing the PBB configurations over time can yield savings of 19.66%.

The solution found by the CG heuristic depends on the value of c^-. For small values of c^-, a large share of aircraft is processed at remote parking positions. With increasing c^-, more PBB capacities are installed to reduce the share of aircraft processed at remote positions. Figure 9 shows the relation between the value of $c^-$and the share of aircraft processed at remote parking positions. Furthermore, the figure presents the total investment, operating and penalty costs obtained depending on the value of c^-. Finally, Table 3 presents the number of gates equipped with each PBB configuration at the beginning of the time horizon and - for each value of c^- - the number of gates equipped with each PBB configuration after the first five time periods.

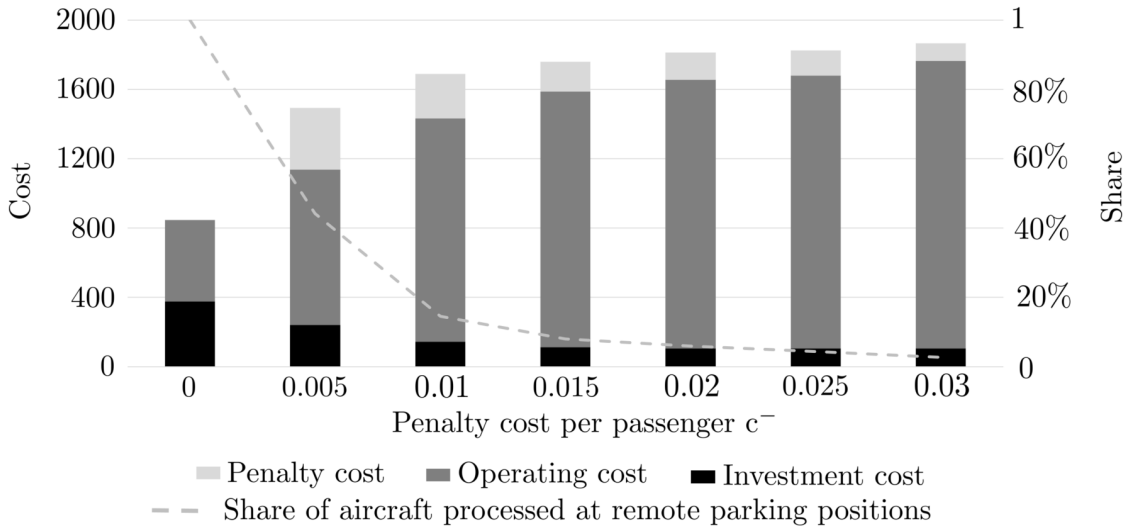

Figure 9: Total investment, operating and penalty costs depending on the value of c^-

In their initial state, as presented in Table 3, the PBB configurations installed at Munich Airport Terminal 2 would allow 98.99% of the traffic modelled for summer 2019 to be accommodated at contact gates. In the light of the given demand scenario, with a strong decrease in demand at the beginning of the time horizon followed by a slow recovery in the following years, PBB configurations are more likely to be downgraded or maintained than upgraded, depending on the ratio of the cost components. As shown in Figure 9, the operating costs are the largest cost item across all values

Table 3: Distribution of PBB configurations at the beginning of the time horizon and after five time periods for each value of c^-

l	$t=0$	$t=5$						
		c^-						
		0	0.005	0.010	0.015	0.020	0.025	0.030
0	0	47	26	13	9	7	6	5
1	27	0	21	28	27	27	28	28
2	15	0	0	6	10	12	12	11
3	1	0	0	0	1	1	1	0
4	4	0	0	0	0	0	0	3

of c^-. For $c^- \in [0; 0.02]$, the operating costs are increasing in c^- and for $c^- \geq 0.02$ they remain comparably constant. Consequently, the higher the value of c^-, the more operating costs are accepted for larger PBB configurations in order to avoid increasing penalty costs. In contrast, the investment costs for changing the configuration are decreasing in c^- for $c^- \in [0; 0.015]$ and remain constant for $c^- \geq 0.015$. That is, the larger the value of c^-, the less gates are downgraded in order to save on operating costs.

In the considered SARS-CoV-2 scenario, PBB configurations are downgraded for all values of c^- (see Table 3). That is, PBB configurations which have the flexibility to accommodate larger types of aircraft are substituted by PBB configurations that can only be used to process smaller types of aircraft. Furthermore, for all values of c^-, the PBB configuration is changed to $l = 0$ at some gates, i.e., the gate is considered a remote parking position after the change. When $c^- = 0$, there is no incentive to accommodate aircraft at contact gates, and in order to reduce the operating costs to the minimum, the PBB configuration is changed to $l = 0$ at all gates in $t = 0$. When c^- is increased to 0.005, the number of gates without any PBBs installed in $t = 5$ decreases to 26. However, no gate remains with $l \geq 2$. The more the value of c^- is increased, the smaller the number of gates without any PBBs after five time periods and the higher the number of gates equipped with $l \geq 2$. Only when $c^- = 0.030$, we observe gates which are equipped with $l = 4$ in $t = 5$. For smaller values of c^-, the high degree of flexibility which justifies the high operating costs of MARS gates cannot be sufficiently exploited in the given traffic scenario.

7.2 Investigating the impact of different budget values

In the remainder of the case study, we investigate the impact of different investment budgets available per period on the solution. Accordingly, we added budget constraints (2c) and run the CG heuristic for budget values $r \in \{0, 8, 16, 32, 64, 1504\}$, where $r = 0$ and $r = 1,504$ represent two extreme scenarios: When $r = 0$, there is no budget available and hence, no PBB configuration changes can be undertaken. By contrast, when $r = 1,504$, the available budget equals the upper bound of the budget demand $G \cdot \max_{k,l \in \mathcal{L}} c^{\mathrm{i}}_{kl}$, and thus, all PBB configuration changes can be undertaken. Based on the prior analysis of the penalty cost, we set c^- to 0.025. Figure 10 shows the resulting total investment, operating, and penalty costs as well as the share of aircraft processed

at remote parking positions for each value of r. Furthermore, Table 4 provides a detailed overview of the investment costs per time period for each value of r. As an example, all results of one instance ($c^- = 0.025$ and $r = 32$) are provided in Appendix C.

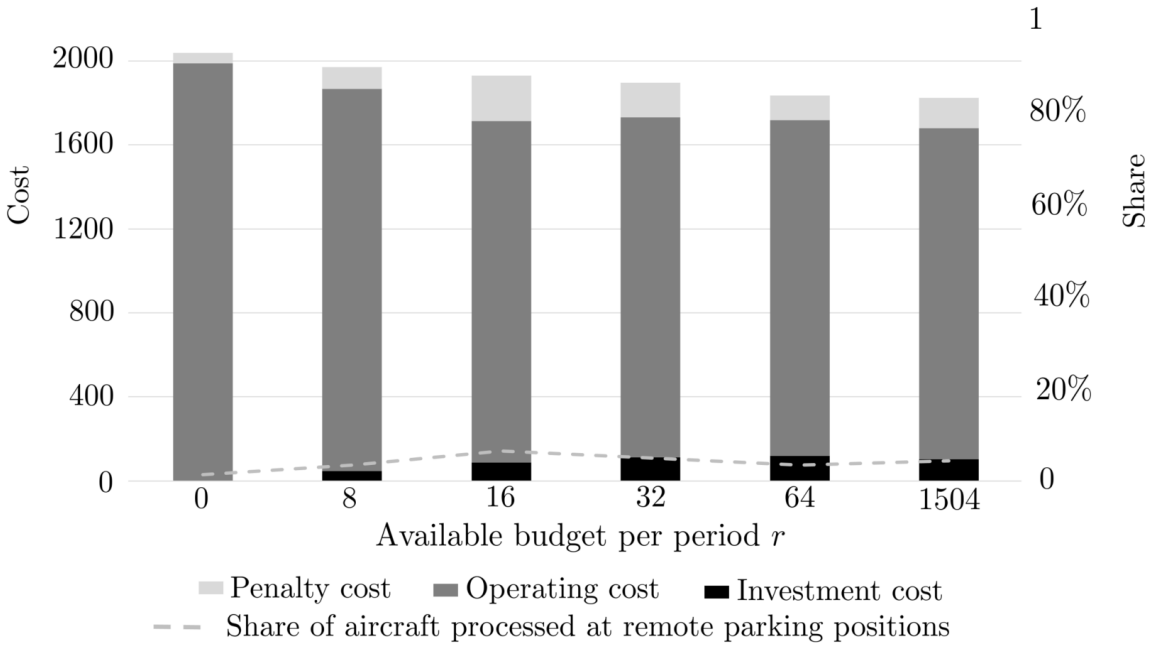

Figure 10: Total investment, operating and penalty costs depending on the value of c^-

Table 4: Investment cost per time period for different values of r

	t																				
r	1	2	3	4	5	6	7	8	9	10	11	12	13	14	15	16	17	18	19	20	$\sum$
0	0	0	0	0	0	0	0	0	0	0	0	0	0	0	0	0	0	0	0	0	0
8	0	0	8	8	8	8	0	8	8	0	0	0	0	0	0	0	0	0	0	0	48
16	16	16	8	16	0	16	0	0	0	8	0	8	0	0	0	0	0	0	0	0	88
32	32	24	16	8	8	0	0	8	0	8	0	0	8	0	0	0	0	0	0	0	112
64	56	24	24	0	0	8	0	0	0	0	8	0	0	0	0	0	0	0	0	0	120
1504	88	8	8	0	0	0	0	0	0	0	0	0	0	0	0	0	0	0	0	0	104

Figure 10 demonstrates that the objective function value improves for higher values of r. The total cost difference between the two extreme scenarios ($r = 0$ and $r = 1,504$) is 10.5%. As discussed earlier, in the SARS-CoV-2 scenario, PBB configurations should be downgraded in order to reduce the operating costs. The higher the available budget for PBB configuration changes is, (1) the more of these changes can be realized, (2) the earlier the changes can be made, and (3) the higher the resulting reduction of operating costs is. The last column of Table 4 shows that higher values of r are associated with higher total investment cost, except for $r = 1,504$. Furthermore, Table 4 shows that the higher the value of r, the more PBB configuration changes tend to be undertaken in early periods of the time horizon where the effect of the change is the largest. Regarding the penalty costs, Figure 10 shows a slight variation in the percentage of aircraft processed at remote parking

positions for different values of r. However, this percentage is smaller than 6.5% in all cases. The maximum is reached for $r = 16$, where the penalty costs also reach their maximum.

Whether a higher budget leads to lower total costs depends on the characteristics of the demand scenario. If the growth in air traffic volume and the change of the fleet mix are moderate, higher budgets will, in general, not lead to considerable savings. By contrast, the SARS-CoV-2 scenario is characterized by a drastic drop in air traffic volume in 2020 and a slow recovery in the following years. Thus, a higher degree of flexibility - especially at the beginning of the time horizon - leads to substantial reductions of total costs.

Overall, the case clarifies the tradeoffs between investment, operating, and penalty costs in a dynamic environment, as well as the relevance of the available investment budget, and demonstrates that our approach provides airports with highly valuable decision support.

8 Conclusions

In this paper, we introduced the dynamic gate configuration problem and formulated it as a deterministic mixed-binary problem. By considering neighborhood constraints, MARS gates and the concept of demand patterns, the mathematical formulation incorporates operational constraints in the strategic context of the problem. Our computational results demonstrated the intractability of the extensive formulation for data instances of realistic size. We presented a CG heuristic to circumvent this problem and illustrated its good performance with respect to solution quality as well as computation time for data instances of mutable complexity. Finally, we presented a case study to demonstrate the implications of the results of the CG heuristic in reality. The results provide important insights for airport managers as to the degree to which the capacities provided at the gates in the present are capable of handling demand during peak hours in the future. Furthermore, the results indicate at *which* gate(s) the PBB configuration should be changed in the event that the solution recommends such change(s). Upgrades are performed such that they maximize the gain in operational flexibility and downgrades are performed such that they minimize the loss of operational flexibility.

In future research, the model could be extended to allow for the addition of new gates within the time horizon, representing terminal extensions or the construction of entirely new terminals. Furthermore, our model does not take into account that managerial decisions besides the ones considered here, not to mention legal constraints, may pose further restrictions on the accommodation of aircraft at certain aircraft stands, besides spatial neighborhood constraints. For example, airports may have mutual agreements with airlines for the exclusive use of gates (for instance, see Young and Wells 2011) and airports may have to provide gates equipped with security equipment of different levels. On the one hand, both aspects require a more detailed subdivision of demand as presented in this paper, while on the other, they might allow a decomposition of the problem. For example, our approach may be applied to a subset of all gates if these gates are used by one airline only by contract and the traffic development can be estimated separately for that airline.

The concept of the model can also be transferred to other problems, where limited capacites need to be (re-)configured to meet changing demand over time. For instance, hospitals have to determine which rooms to allocate to which ward, while the number of patients treated by the wards fluctuates over time and both investment and personnel costs need to be considered.

References

Aena (2020) *Guía de tarifas 2020 (tariff guide 2020): Edición octubre (edition october)*. URL http://www.aena.es/es/comercial/guia-tarifas.html.

Airbus (2018) *Global market forecast: Global networks, global citizens: 2018-2037*. URL https://www.airbus.com/content/dam/corporate-topics/publications/media-day/GMF-2018-2037.pdf.

Airbus (2019) *Airbus and emirates reach agreement on a380 fleet, sign new widebody orders*. URL https://www.airbus.com/newsroom/press-releases/en/2019/02/airbus-and-emirates-reach-agreement-on-a380-fleet--sign-new-widebody-orders.html.

Airport Cooperative Research Program (2010) *Airport passenger terminal planning and design: Volume 1: Guidebook*. URL http://jetchico.org/wp-content/uploads/2016/06/Airport-Passenger-Terminal-Planning-and-Design-vol-1.pdf.

Airport Improvement Magazine (2010) *"like new" boarding bridges return to service at daytona beach*. URL https://airportimprovement.com/article/new-boarding-bridges-return-service-daytona-beach.

Ashford NJ, Mumayiz SA, Wright PH, eds. (2011) *Airport Engineering: Planning, Design, and Development of 21st Century Airports* (Hoboken, New Jersey: John Wiley & Sons), 4th edition.

Bandara SJ, Wirasinghe SC (1989) *Airport gate position estimation under uncertainty. Transportation Research Record Journal of the Transportation Research Board* 1199:41–48.

Boeing (2020) *Boeing ceo updates employees on quarterly results and market realities*. URL https://boeing.mediaroom.com/news-releases-statements?item=130713.

Boston Consulting Group (2020) *Seven trends that will reshape the airline industry*. URL https://www.bcg.com/publications/2020/seven-trends-reshape-airline-industry.

Caves R (1994) *A search for more airport apron capacity. Journal of Air Transport Management* 1(2):109–120.

Cheng CH, Ho SC, Kwan CL (2012) *The use of meta-heuristics for airport gate assignment. Expert Systems with Applications* 39(16):12430–12437.

Daş GS, Gzara F, Stützle T (2020) *A review on airport gate assignment problems: Single versus multi objective approaches. Omega* 92:102–146.

de Neufville R, Odoni AR (2013) *Airport Systems: Planning, Design, and Management* (New York: McGraw-Hill).

Desrosiers J, Lübbecke ME (2005) *A primer in column generation*. Desaulniers G, Desrosiers J, Solomon MM, eds., *Column Generation*, 1–32 (New York: Springer US).

Dorndorf U, Drexl A, Nikulin Y, Pesch E (2007) *Flight gate scheduling: State-of-the-art and recent developments. Omega* 35(3):326–334.

Dorndorf U, Jaehn F, Pesch E (2017) *Flight gate assignment and recovery strategies with stochastic arrival and departure times. OR Spectrum* 39(1):65–93.

Eurocontrol (2018) *European aviation in 2040: Challenges of growth*. URL https://www.eurocontrol.int/sites/default/files/content/documents/official-documents/reports/challenges-of-growth-2018.pdf.

Guépet J, Acuna-Agost R, Briant O, Gayon JP (2015) *Exact and heuristic approaches to the airport stand allocation problem. European Journal of Operational Research* 246(2):597–608.

Hagspihl T, Kolisch R, Ruf C, Schiffels S (2021) *Case study data for: "dynamic gate configurations at airports: A network optimization approach". Mendeley Data* (V1).

Hassounah MI, Steuart GN (1993) *Demand for aircraft gates. Transportation Research Record* 1423(1423):26–33.

Horonjeff R, McKelvey FX, Sproule WJ, Young SB (2010) *Planning and Design of Airports* (New York: McGraw-Hill), 5th edition.

International Air Transport Association (2004) *Airport development reference manual: 9th edition effective january 2004*. URL `https://www.iata.org/en/publications/store/airport-development-reference-manual/`.

International Civil Aviation Organization (2005) *Doc 9157 aerodrome design manual: Part 2: Taxiways, aprons and holding bays*. URL `https://www.bazl.admin.ch/dam/bazl/de/dokumente/Fachleute/Flugplaetze/ICAO/icao_doc_9157_aerodromedesignmanual-part2.pdf.download.pdf/icao_doc_9157_aerodromedesignmanual-part2.pdf`.

International Civil Aviation Organization (2018) *Annex 14 to the convention on international civil aviation: Aerodromes: Volume 1 aerodrome design and operations*. URL `https://www.bazl.admin.ch/dam/bazl/de/dokumente/Fachleute/Regulationen_und_Grundlagen/icao-annex/icao_annex_14_aerodromesvolumei-aerodromedesignandoperations.pdf.download.pdf/an14_v1_cons.pdf`.

Kazda A, Caves RE (2008) *Airport Design and Operation* (Bingley: Emerald), 2nd edition.

Mirković B, Tošić V (2014) *Airport apron capacity: estimation, representation, and flexibility. Journal of Advanced Transportation* 48(2):97–118.

Mirković B, Tošić V (2017) *The difference between hub and non-hub airports – an airside capacity perspective. Journal of Air Transport Management* 62:121–128.

Morabit M, Desaulniers G, Lodi A (2020) *Machine-learning-based column selection for column generation. Technical report, Les Cahiers du GERAD G–2020–29* .

Munich Airport (2016) *Münchner flughafen plant die erweiterung von terminal 1 (munich airport is planning the extension of terminal 1)*. URL `https://www.munich-airport.de/mehr-kapazitat-mehr-qualitat-mehr-komfort-338570`.

Munich Airport (2020) *Annual traffic report 2019*. URL `https://www.munich-airport.com/_b/0000000000000008934656bb5e9eb677/annual-traffic-report-2019.pdf`.

Narciso ME, Piera MA (2015) *Robust gate assignment procedures from an airport management perspective. Omega* (50):82–95.

Steuart GN (1974) *Gate position requirements at metropolitan airports. Transportation Science* 8(2):169–189.

Travel PR News (2019) *Budapest airport installs brand new passenger boarding bridges*. URL `https://travelprnews.com/budapest-airport-installs-brand-new-passenger-boarding-bridges-649599/travel-press-release/2019/05/27/`.

Wirasinghe SC, Bandara SJ (1990) *Airport gate position estimation for minimum total costs—approximate closed form solution. Transportation Research Part B: Methodological* 24(4):287–297.

Young SB, Wells AT (2011) *Airport Planning & Management* (New York, NY: McGraw-Hill), 6th edition.

Appendix A Notation

Table 5: Notation

Sets, parameter		
$\mathcal{T} = \{0, \ldots, T\}$		Planning horizon
$\mathcal{L} = \{0, \ldots, L\}$		PBB configurations
$\mathcal{A} = \{1, \ldots, A\}$		Aircraft classes
$\mathcal{G} = \{1, \ldots, G\}$		Aircraft stands
$\mathcal{J} = \{1, \ldots, J\}$		Lead-in lines
$\mathcal{B} = \{1, \ldots, B\}$		Demand patterns
s_a	[meters]	Maximum half wingspan of aircraft belonging to class $a \in \mathcal{A}$ including additional space for minimum separation requirements
d_{ij}	[meters]	Lateral distance between lead-in lines $i \in \mathcal{J}$ and $j \in \mathcal{J}$
$\mathcal{J}_g$		Set containing all lead-in lines belonging to gate $g \in \mathcal{G}$
$\mathcal{N}_g$		Set containing gate $g \in \mathcal{G}$ and its dexter neighbor gate
$\mathcal{L}_a$		PBB configurations that can be used to accommodate aircraft class $a \in \mathcal{A}$
p_a		Average number of passengers on board an aircraft of class $a \in \mathcal{A}$
$\mathcal{L}^{MARS}$		PBB configurations which indicate a MARS configuration
c^{i}_{kl}	[MU's[14]]	Investment cost of PBB configuration $l \in \mathcal{L}$, if PBB configuration $k \in \mathcal{L}$ is currently installed
c^{o}_{l}	[MU's]	Operating cost of PBB configuration $l \in \mathcal{L}$
c^{-}	[MU's]	Penalty cost per passenger
e_{gtl}		1, if aircraft stand $g \in \mathcal{G}$ has PBB configuration $l \in \mathcal{L}$ installed in period $t = 0$; 0, otherwise
D_{ba}		Demand of aircraft class $a \in \mathcal{A}$ according to demand pattern $b \in \mathcal{B}$
r_t	[MU's]	Available investment budget in period $t \in \mathcal{T}$
$\mathcal{B}_t$		Demand patterns of period $t \in \mathcal{T}$
f_{tb}		Relative weight of demand pattern $b \in \mathcal{B}$ in period $t \in \mathcal{T}$
M		Sufficiently large number
Decision variables		
$z_{gtl} \in \{0, 1\}$		1, if PBB configuration $l \in \mathcal{L}$ is installed at aircraft stand $g \in \mathcal{G}$ in period $(t, t+1)$ for $t = 0, \ldots, T-1$; 0, otherwise

[14] MU = monetary unit

$x_{gtkl} \in \{0,1\}$	1, if PBB configuration $l \in \mathcal{L}$ is built at aircraft stand $g \in \mathcal{G}$ starting with PBB configuration $k \in \mathcal{L} \setminus \{l\}$ at time $t = 0, \ldots, T-1$; 0, otherwise
$y_{gjtba} \in \{0,1\}$	1, if aircraft stand $g \in \mathcal{G}$ (lead-in line $j \in \mathcal{J}$) is used for aircraft of class $a \in \mathcal{A}$ in period $(t, t+1)$ for demand pattern $b \in \mathcal{B}_t$; 0, otherwise
$y^-_{tba} \geq 0$	Uncovered demand in period $(t, t+1)$ for $t = 0, \ldots, T-1$ for aircraft of class $a \in \mathcal{A}$ for demand pattern $b \in \mathcal{B}_t$

Table 6: Additional notation for column generation approach

Sets, parameter		
$\mathcal{P} = \{1, \ldots, P\}$		Paths (for all aircraft stands $g \in \mathcal{G}$)
$\mathcal{P}_g$		Paths associated with aircraft stand $g \in \mathcal{G}$
c_p	[MU's]	Total (investment and operating) cost of path $p \in \mathcal{P}$
z^p_{gtl}		1, if PBB configuration $l \in \mathcal{L}$ is installed at aircraft stand $g \in \mathcal{G}$ in period $(t, t+1)$ for $t = 0, \ldots, T-1$ in path $p \in \mathcal{P}$; 0 otherwise
$\pi^{\text{cap,line}}_{jtb}$		Dual variable of the respective (lead-in line) capacity constraint in the master problem
$\pi^{\text{cap,gate}}_{tb}$		Dual variable of the respective (gate) capacity constraint in the master problem
π^{com}_{jtba}		Dual variable of the respective compatibility constraint in the master problem
π^{con}		Dual variable of the respective convexity constraint in the master problem
Decision variables		
$\lambda_p \in \{0,1\}$		1, if path $p \in \mathcal{P}$ is used; 0, otherwise

Appendix B Allocation of Demand Patterns to Time Periods

Depending on the number of gates G, we pre-define a set of $B = 10$ demand patterns as

$$D_{ba} = \begin{pmatrix} 1.2 \cdot G & 0 & 0 \\ G & 0.1 \cdot G & 0 \\ 0.9 \cdot G & 0.05 \cdot G & 0.05 \cdot G \\ 0.9 \cdot G & 0 & 0.1 \cdot G \\ 0.5 \cdot G & 0.4 \cdot G & 0 \\ 0.5 \cdot G & 0.25 \cdot G & 0.05 \cdot G \\ 0.5 \cdot G & 0.2 \cdot G & 0.1 \cdot G \\ 0.5 \cdot G & 0 & 0.2 \cdot G \\ 0.25 \cdot G & 0.25 \cdot G & 0.25 \cdot G \\ 0.25 \cdot G & 0.15 \cdot G & 0.35 \cdot G \end{pmatrix}.$$

The matrix is defined such that a higher value of b corresponds with a higher share of large and very large aircraft. We allocate the demand patterns to time periods according to the following scheme:

- If $t \leq \frac{T}{3}$: Randomly allocate three demand patterns from the subset of demand patterns in $\mathcal{B}$ with index $[0; 4]$ to time period t
- If $t > \frac{T}{3}$ and $t \leq \frac{2 \cdot T}{3}$: Randomly allocate three demand patterns from the subset of demand patterns in $\mathcal{B}$ with index $[3; 7]$ to time period t
- Else: Randomly allocate three demand patterns from the subset of demand patterns in $\mathcal{B}$ with index $[6; 9]$ to time period t

Appendix C Case Study: Detailed Results for $c^- = 0.025$ and $r = 32$

In the following we present detailed results for the case study provided in Section 7 with $c^- = 0.025$ and $r = 32$. Table 8 provides the PBB configurations for each gate $g \in \mathcal{G}$ and time period $t \in \mathcal{T}$. PBB configuration changes are highlighted for visibility. When the PBB configuration of a gate is downgraded, the respective cell is dyed gray. When it is upgraded, the cell is enframed.

Table 8: Resulting PBB configurations at Munich Airport for $c^- = 0.025$ and $r = 32$

	t																				
g	0	1	2	3	4	5	6	7	8	9	10	11	12	13	14	15	16	17	18	19	20
0	2	2	2	2	2	2	2	2	2	2	2	2	2	2	2	2	2	2	2	2	2
1	1	1	1	1	1	1	1	1	1	1	1	1	1	1	1	1	1	1	1	1	1
2	1	1	1	1	1	1	1	1	1	1	1	1	1	1	1	1	1	1	1	1	1
3	2	2	2	2	2	2	2	2	1	1	1	1	1	1	1	1	1	1	1	1	1
4	1	1	1	1	1	1	1	1	1	1	1	1	1	1	1	1	1	1	1	1	1
5	1	1	0	0	0	0	0	0	0	0	0	0	0	0	0	0	0	0	0	0	0
6	2	2	2	2	2	2	2	2	2	2	2	2	2	2	2	2	2	2	2	2	2
7	1	1	1	1	1	1	1	1	1	1	1	1	1	1	1	1	1	1	1	1	1
8	2	2	2	2	2	2	2	2	2	2	2	2	2	2	2	2	2	2	2	2	2
9	1	0	0	0	0	0	0	0	0	0	0	0	0	0	0	0	0	0	0	0	0
10	1	1	1	1	1	1	1	1	1	1	1	1	1	1	1	1	1	1	1	1	1
11	1	1	1	0	0	0	0	0	0	0	0	0	0	0	0	0	0	0	0	0	0
12	1	1	1	1	1	1	1	1	1	1	1	1	1	1	1	1	1	1	1	1	1
13	2	2	2	2	2	2	2	2	2	2	2	2	2	2	2	2	2	2	2	2	2
14	1	1	1	1	1	1	1	1	1	1	1	1	1	1	1	1	1	1	1	1	1
15	2	2	2	2	2	2	2	2	2	2	2	2	2	2	2	2	2	2	2	2	2
16	1	1	1	1	1	1	1	1	1	1	1	1	1	1	1	1	1	1	1	1	1
17	1	1	1	0	0	0	0	0	0	0	0	0	0	0	0	0	0	0	0	0	0
18	2	2	2	2	2	2	2	2	2	2	2	2	2	2	2	2	2	2	2	2	2
19	1	1	1	1	1	1	1	1	1	1	1	1	1	1	1	1	1	1	1	1	1
20	1	1	1	1	1	1	1	1	1	1	1	1	1	1	1	1	1	1	1	1	1
21	2	2	2	2	2	2	2	2	2	2	2	2	2	2	2	2	2	2	2	2	2
22	1	1	1	1	1	1	1	1	1	1	1	1	1	1	1	1	1	1	1	1	1
23	2	2	2	2	2	2	2	2	2	2	2	2	2	2	2	2	2	2	2	2	2
24	1	1	1	1	1	1	1	1	1	1	1	1	1	1	1	1	1	1	1	1	1
25	2	2	2	2	2	2	2	2	2	2	2	2	2	2	2	2	2	2	2	2	2
26	1	1	1	1	1	1	1	1	1	1	1	1	1	1	1	1	1	1	1	1	1
27	2	2	2	2	2	2	2	2	2	2	2	2	2	2	2	2	2	2	2	2	2
28	1	1	1	1	1	1	1	1	1	1	1	1	1	1	1	1	1	1	1	1	1
29	2	2	2	2	2	2	2	2	2	2	2	2	2	2	2	2	2	2	2	2	2
30	3	1	1	1	1	1	1	1	1	1	1	1	1	1	1	1	1	1	1	1	1
31	2	2	0	0	0	0	0	0	0	0	0	0	0	0	0	0	0	0	0	0	0
32	1	1	1	1	1	1	1	1	1	1	1	1	1	1	1	1	1	1	1	1	1
33	2	2	2	2	2	1	1	1	1	1	1	1	1	1	1	1	1	1	1	1	1
34	1	1	1	1	1	1	1	1	1	1	1	1	1	1	1	1	1	1	1	1	1
35	2	0	0	0	0	0	0	0	0	0	0	0	0	1	1	1	1	1	1	1	1
36	1	1	1	1	1	1	1	1	1	1	1	1	1	1	1	1	1	1	1	1	1
37	4	1	1	1	1	1	1	1	1	1	1	1	1	1	1	1	1	1	1	1	1
38	4	4	1	1	1	1	1	1	1	1	1	1	1	1	1	1	1	1	1	1	1
39	1	1	1	1	1	1	1	1	1	1	1	1	1	1	1	1	1	1	1	1	1
40	1	1	1	1	1	1	1	1	1	1	1	1	1	1	1	1	1	1	1	1	1
41	1	1	1	1	1	1	1	1	1	1	1	1	1	1	1	1	1	1	1	1	1
42	1	1	1	1	1	1	1	1	1	1	1	1	1	1	1	1	1	1	1	1	1
43	1	1	1	1	1	1	1	1	1	1	1	1	1	1	1	1	1	1	1	1	1
44	1	1	1	1	1	1	1	1	1	1	1	1	1	1	1	1	1	1	1	1	1
45	4	4	4	4	4	4	4	4	4	4	2	2	2	2	2	2	2	2	2	2	2
46	4	4	4	4	3	3	3	3	3	3	3	3	3	3	3	3	3	3	3	3	3